Mathematical Biosciences and Engineering

https://www.aimspress.com/journal/mbe

MBE, 23(4): 1121–1155.
DOI: 10.3934/mbe.2026042
Received: 25 September 2025
Revised: 05 January 2026
Accepted: 08 January 2026
Published: 11 March 2026

Research article

Data-driven modeling of imported malaria in Morocco and the impact of population migration

Hamza Toufga[1], Ghassane Benrhmach[2], Mustapha Lhous[1] and Abdessamad Tridane[3,*]

[1] Laboratory of Mathematical Analysis, Algebra and Applications (LAM2A), Department of Mathematics and Computer Science, Faculty of Sciences Ain Chock, Hassan II University of Casablanca, Morocco

[2] Department of Mathematics & Statistics, College of Engineering, Abu Dhabi University, Abu Dhabi, United Arab Emirates

[3] Department of Mathematics, College of Science, United Arab Emirates University, Al Ain, United Arab Emirates

* **Correspondence:** Email: a-tridane@uaeu.ac.ae.

Abstract: Malaria remains a very critical health-threatening issue worldwide, and increasingly, migration is viewed as a cause of re-emergence in malaria-free zones. This study proposes a data-driven, deterministic compartmental model that explicitly accounts for human immigration when modeling malaria transmission from humans to mosquito populations. The human host is categorized into susceptible, asymptomatic, infected, and recovered classes, while the vector population is stratified into susceptible and infected compartments. The paper presents a rigorous mathematical analysis to prove the positivity and uniqueness of solutions, and further demonstrates that the model only admits a globally stable endemic equilibrium. Using Morocco as a case study, key parameters are estimated using three complementary methods: least-squares fit, Extended Kalman Filter, and Long Short-Term Memory (LSTM) neural networks, which where applied to imported malaria data from 1990 through 2023. To identify the best control measures to prevent the possible re-establishment of malaria in Morocco, we investigate an optimal control problem that includes awareness, prophylactic treatment, treatment of the infected population, and vector control with insecticide. The goal is to identify the optimal effectiveness of these controls. Numerical results show a significant reduction in human and vector infections through a combination of control strategies, thus underscoring the importance of surveillance and control policies that account for migration. Therfore, it serves as a practical, flexible framework to analyze imported malaria and other vector-borne diseases across similarly high-mobility areas.

Keywords: imported malaria; human migration; estimation of parameters; optimal control; Pontryagin's maximum principle; numerical simulation

1. Introduction

Malaria has consistently been a major public health concern for several years and continues to impose a heavy load on global health care systems, most especially within sub-Saharan Africa. The condition is caused by the protozoan parasites of the genus *Plasmodium* being transmitted to humans by the female *Anopheles* mosquitoes that are already infected [1]. Quoting from the World Health Organisation (WHO)and World Malaria Report 2024, most malaria morbidity worldwide is in the African region: the continent registered approximately 246 million cases around 2023, with over 500,000 deaths, thus representing about 94% of the global morbidity and nearly 95% of all malaria deaths [2].

Individually, Nigeria and the Democratic Republic of the Congo carry the heaviest burden, with Nigeria alone accounting for above 25% of all global cases and almost 30% of human deaths due to malaria, whilst the Democratic Republic of the Congo accounts for about 12% of global malaria cases and 11% of global malaria deaths [1, 3–8].

Not only threatening public health, malaria imposes a significant economic burden on the host countries. In Brazil, malaria sufferers lose an average of two working days. In India, this figure goes up to eleven. Moreover, an average of over nine workdays are lost in Ivory Coast, thus leading to lower household income and an above-average level of poverty. Consequently, the affected families are compelled to borrow and pawn resources in order to afford malaria-related treatments and preventive measures [9]. Such adverse feedbacks are widely articulated in the literature under the very idea of amplification of deprivation, and results in poorer populations being disproportionately affected by the limited access to important interventions, including Insecticide-Treated bed Nets (ITNs), early diagnoses, and effective treatments. The situation is further worsened where housing conditions are poor, therby encouraging abundant stagnant waters and hence more ideal breeding sites for mosquitoes to thrive. Therefore, Malaria is a further negative factor for tourism, a disincentive to investments, and impedes economic development in high-endemic regions [9–11]. Therefore, the control of malaria requires medical interventions and comprehensive socioeconomic strategies. A few decades rolling down the road, the concerted efforts of the WHO, academia, and authorities at local or community levels, through funds, awareness campaigns, and large-scale net distribution, have significantly increased the field of prevention, particularly in the rural areas of Africa [2, 5, 12, 13]. Due to these collective endeavors, the success story of WHO-certified malaria-free countries is increasingly possible for many nations that were previously gravely affected.

However, the context of rapid mobility, displacement, and migration continues to make the attainment of universal health coverage fragile [2, 4]. Temporary or permanent human movement poses a significant risk of reintroduction of malaria into regions that had achieved local transmission elimination and its spread to regions that were previously unaffected. The highest risk occurs when the population movement matches with the presence of competent mosquito vectors [14]. For example, 2022 European Union annual reports on malaria surveillance found that travel occurred in 99.8% of over 6000 confirmed malaria cases, mainly from West Africa [15]. A comparable situation was seen in a study within Spain's ranks between the years 2002–2015, which identified that almost all the reported malaria cases were imported, chiefly from Africa and Asia [16]. Equally, Mexico saw a rise in imported malaria cases associated with movement, mainly from Guinea and several Central American countries.

Morocco is an appropriate study of the issue of the persistence of human migration to the area. Malaria-free status was granted to the country by the WHO as of 2010, but there nevertheless remained a number of importations. Over 50 imported malaria cases were registered in Tangier–Tetouan–Al Hoceima alone, mainly from Guinea, Mali, and the Ivory Coast [17]. In line with this, similar patterns were seen at the Ibn Sina Hospital in Rabat [18]. Indeed, imported malaria persists due to migration trajectories into Morocco through the south and the border located in Guerguerat, connecting sub-Saharan Africa with the northern territories and subsequently with Europe through Tangier Med. While migration is largely legal in the books, the true scale of migration might be vastly underestimated because of illegal routes being traversed. Initially intending to travel through Morocco, most immigrants now have to endure longer stays, thereby settling in localities where *Anopheles* mosquitoes have inhabited findable places [19]. Hence, it reinforces recognition of the role of human movements in sustaining cases of imported malaria and identifying any risk of residual malaria transmission in regions exchanged by malaria eradication [20]. The climate amplifies this risk even more. The latest studies revealed that sufficiently large areas of not only the north of Morocco but central Morocco are already suitable for *Anopheles multicolor* and *Anopheles sergentii*; climate change may shift their distributions further northward and upward to higher altitudes by 2050 [21]. Such climate-driven alterations in the distribution of vectors would raise the probabilities for malaria's reintroduction [22], thus highlighting the need for robust surveillance systems in Morocco.

Mathematical modeling is crucial to understand and predict the transmission dynamics of malaria. The foundation of malaria modeling was established by Ross [23], who linked mosquito life cycles to infection processes. Macdonald [24] included mosquito biology and showed that reducing the mosquito density can influence the transmission. Dietz et al. [25] examined the role of human immunity in controlling the transmission and introduced an exposed compartment to account for any pre-infectious latency. More recent research has applied many optimal control theories into malaria dynamics, such as the study by Abioye et al. [26], which focused on interventions in pregnant women and newborns, and Otieno et al. [27] , which addressed control strategies in endemic regions of Kenya. The study by Kim et al. [28] evaluated the efficiency of border-screening interventions, while Yacheur et al. [29] evaluated immigration's impact on malaria dynamics in North African countries. A more recent study conducted by Rajnarayanan et al. [30] proposed climate-dependent models of malaria risk based on temperature and geographic altitude with the use of physics-informed neural networks, thereby estimating country-level malaria risk indicators on the African continent.

There is a lack of literature that focuses on malaria transmission due to immigration factors in countries where malaria transmission exists. Striking examples of such conditions include the influx of malaria cases from the South African continent into Morocco, as depicted in Figure 1. Indeed, the increasing number of imported malaria cases exacerbates the necessity of studying how migration from sub-Saharan Africa might endanger the malaria-free status of countries such as Morocco. To the best of our knowledge, this study which focuses on the reintroduction of malaria in a malaria-free country, is the first of its kind in the context of mathematical modeling coupled with data-based parameter estimation methods.

The rest of this article is organized as follows: the dynamical model is described in Section 2, where the positivity, existence, and invariant sets are established in Section 3; Section 4 discusses the endemic equilibrium, while Section 5 examines the global stability; then, the parameter estimation is

carried out in Section 6 using least-squares, Kalman filter, and Long Short Term Memory (LSTM) methods with Moroccan data from 1990 to 2023 in Section 7; afterward, optimal control with four different control strategies is explored in Section 8; and the conclusion with policy implications is presented in Section 9.

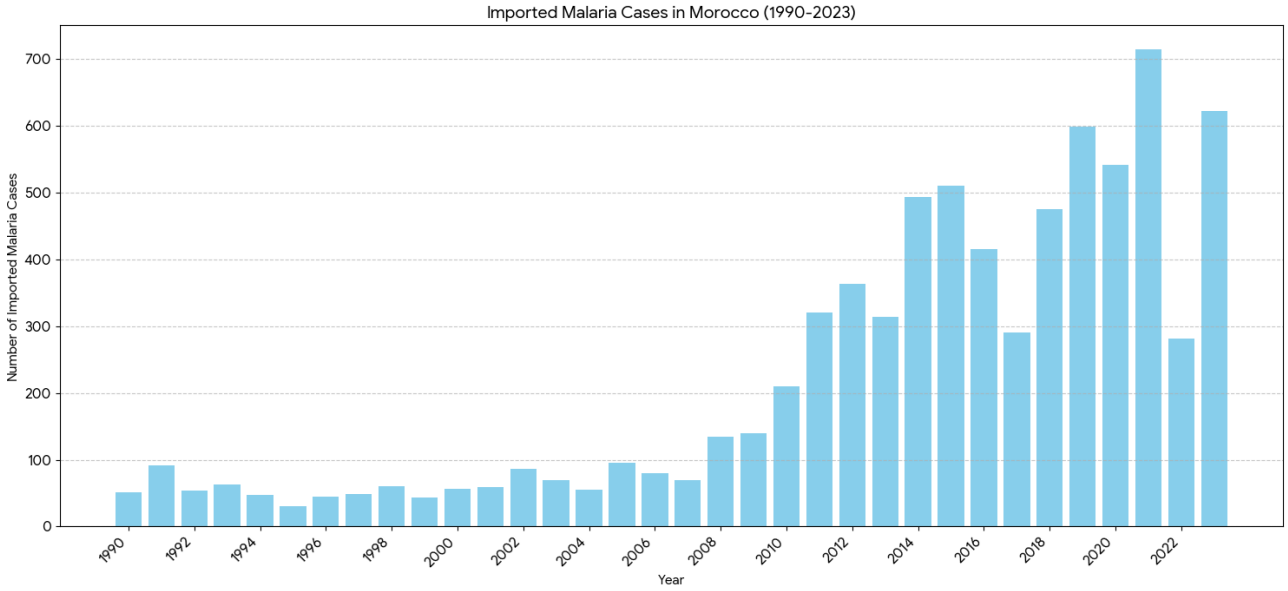

Figure 1. Imported malaria cases in Morocco from 1990 to 2023.

2. Description and analysis of malaria model

We formulate a compartment-based deterministic model to capture the dynamics of malaria in a population subject to immigration as follows:

$$\frac{dS}{dt} = \Lambda_S - d_S S - \beta_1 S I_V, \tag{2.1}$$

$$\frac{dA}{dt} = \Lambda_A - (d_A + \theta)A + \varepsilon\beta_1 S I_V, \tag{2.2}$$

$$\frac{dI}{dt} = (1-\varepsilon)\beta_1 S I_V + \theta A - (\gamma + d_I + \alpha)I, \tag{2.3}$$

$$\frac{dR}{dt} = \Lambda_R - d_R R + \gamma I, \tag{2.4}$$

$$\frac{dS_V}{dt} = \Lambda_V - \beta_2 S_V (A + \kappa I) - d_V S_V, \tag{2.5}$$

$$\frac{dI_V}{dt} = \beta_2 S_V (A + \kappa I) - d_V I_V, \tag{2.6}$$

where

$$S(0) = S_0, \quad A(0) = A_0, \quad I(0) = I_0, \quad R(0) = R_0,$$
$$S_V(0) = S_{V0}, \quad I_V(0) = I_{V0}.$$

The human host population is subdivided into four classes: susceptible (S), asymptomatic or partially immune (A), actively infected (I), and recovered (R). Susceptible individuals enter the population at a constant rate, and this rate also represents the immigration of the susceptible population, denoted by Λ_S. We suppose that the susceptible people S are those who are not yet infected with malaria but can become infected when they come into contact or interact with infected vectors I_V. At a rate of $\varepsilon\beta_1 SI_V$, susceptible individuals S can also progress into the asymptomatic compartment of humans, where ε represents human immunity. These asymptomatic compartments are classified as infected humans, having a symptomatic and infectious disease. These individuals can move to an active malaria infection at a rate θ. Additionally, susceptible humans, S, can directly progress into infected persons, which explains the rise in the number of infected people at a rate of $(1-\varepsilon)\beta_1 SI_V$. Moreover, this compartment of infected people can move to the recovered class at a rate γ and death due to the infection by a rate α. The population of vectors can be infected when susceptible vectors S_V interact with asymptomatic humans at rate β_2 or with infected humans at rate $\beta_2\kappa$. Additionnaly, each compartment is subject to natural death: susceptible humans at rate d_S, infected at d_I, and recovered at d_R. Similarly, for the second population (vectors), susceptible S_V and infected I_V die at rate d_V. Additionally, Λ_A and Λ_R represent the immigration rates for asymptomatic and recovered humans, respectively. In parallel, the vector population is divided into susceptible (S_V) and infected (I_V) compartments, with new vectores entering S_V at a constant rate (Λ_V). Susceptible vectors become infected upon biting asymptomatic or infected humans, and infected vectors do not recover. Notably, immigration augments both S and A compartments, thereby reflecting the movement of potentially susceptible or partially immune individuals from endemic regions. These mechanisms are in harmony with the modeling studies that indicate that the presence of partially immune individuals and protected travelers could significantly change the transmission routes and the effectiveness of interventions in malaria systems [31]. Thus, the resulting system of six ordinary differential equations characterizes how human vector interactions and migration jointly shape malaria transmission. Models with similar structures that include demographic heterogeneity, ageing, or resusceptibility have been successfully used in recent epidemics, which clearly demonstrates the significance of demographic structure in determining the long-term transmission dynamics [32]. The flow chart of the proposed model is given in Figure 2.

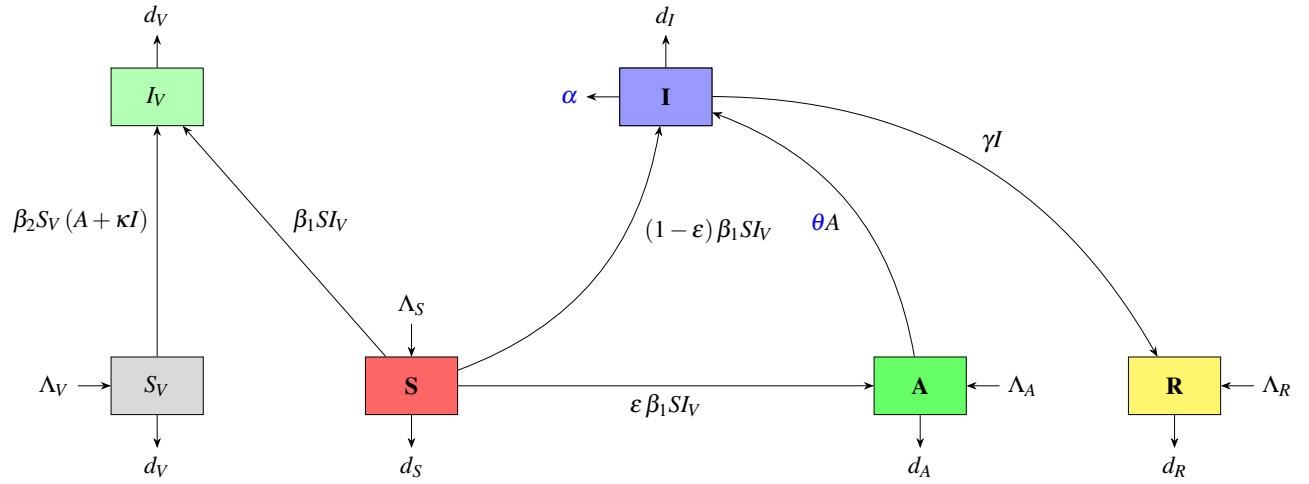

Figure 2. Flow chart of malaria models (2.1)–(2.6) with human migration.

It is assumed that all parameters have positive values, whereas the values of $\Lambda_S, \Lambda_A, \Lambda_R$, and Λ_V are also positive. Table 1 presents the model's parameter definitions based on their biological meaning.

Table 1. Biological parameters and their values.

Parameter	Description	Value	Source
Λ_S	Immigration rate of susceptible humans	0.3	[33, 34]
Λ_A	Immigration rate of asymptomatic humans	0.3	Assumed
Λ_R	Immigration rate of recovered humans	0.1	Assumed
Λ_V	Recruitment rate of susceptible vectors	0.18898	[30]
d_S	Natural death rate of susceptible humans	0.0023069281	Fitted
d_A	Natural death rate of asymptomatic humans	0.00284968	Fitted
d_I	Natural death rate of infected humans	0.001247093	Fitted
d_R	Natural death rate of recovered humans	0.000100	Fitted
d_V	Natural death rate of vectors	0.0000309	Fitted
β_1	Human infection rate from infected vectors	0.000001817384	Fitted
β_2	Vector infection rate from infected/asympt. humans	0.0003084285	Fitted
γ	Recovery rate of infected humans	0.00414752	Fitted
θ	Progression rate from A to I	0.100815	Fitted
α	Malaria-induced mortality rate	0.04	Fitted
κ	Enhancement factor for infectious humans	0.03	Fitted
ε	Human immunity level	0.6941	Fitted

3. Basic properties of the model

First, we aim to show the basic properties of the model. (i.e., the solutions of models (2.1)–(2.6) remain positive and bounded when starting from non-negative initial conditions). In fact, we have the following result.

Theorem 3.1. *Assuming that the initial conditions* $S(0), A(0), I(0), R(0), S_V(0)$ *, and* $I_V(0)$ *are positive, the solutions of systems* (2.1)–(2.6) *are positive for all* $t \geq 0$.

To show the existence of the solution , we have the following theorem.

Theorem 3.2. *Systems* (2.1)–(2.6) *that fulfill the given initial conditions* $S(0), A(0), I(0), R(0), S_V(0)$, *and* $I_V(0)$ *has a unique solution.*

3.1. Invariant region

Theorem 3.3. *The set*

$$\mathscr{E} = \left\{(S, A, I, R, S_V, I_V) \in \mathbb{R}^6_+ : N \leq \frac{\Lambda_S + \Lambda_A}{\zeta}, N_V \leq \frac{\Lambda_V}{d_V}\right\}$$

is positively invariant under systems (2.1)–(2.6) *with initial conditions* $S(0)$, $A(0)$, $I(0)$, $R(0)$, $S_V(0)$, *and* $I_V(0)$, *where* $\zeta = \max\{d_A, d_I, d_S, d_R\}$.

4. Analysis of the mathematical model

To examine the progression of Malaria dynamics, we construct the model in (2.1)–(2.6), thereby explicitly incorporating a continuous influx of immigrants into the population. Because these arrivals introduce potentially infected individuals, the system does not admit a disease-free equilibrium. Instead, our investigation centers on the model's unique endemic equilibrium, which remains the sole steady state. Establishing the global stability of this endemic equilibrium constitutes one of the principal results of our analysis. In the remainder of this section, we detail the theoretical underpinnings of the equilibrium and prove its global stability in the following theorem.

Theorem 4.1. *Systems* (2.1)–(2.6) *has no malaria-free equilibrium, but admits an endemic equilibrium point.*

5. Global stability

The following assumptions constitute sufficient conditions for the global asymptotic stability of the endemic equilibrium of systems (2.1)–(2.6)

$(\mathbf{H}_1)$ $\dfrac{\theta\kappa}{\gamma + d_I + \alpha} < 1.$

$(\mathbf{H}_2)$ $\left(\frac{I^*}{I} - 1\right)\left(\frac{A}{A^*} - 1\right) \geq 0$ and $\left(\frac{I^*}{I} - 1\right)\left(\frac{SI_V}{S^*I_V^*} - 1\right) \geq 0.$

Theorem 5.1. *Assume* $(\mathbf{H}_1)$ *and* $(\mathbf{H}_2)$ *hold. The endemic equilibrium point is globally asymptotically stable in* $\mathscr{E}$.

6. Estimation of parameters

Table 2. Imported malaria cases in Morocco from 1990 to 2023 and their sources.

Year	Number of Cases	Source
1990	51	[35]
1991	91	[35]
1992	54	[35]
1993	63	[35]
1994	48	[35]
1995	31	[35]
1996	45	[35]
1997	49	[35]
1998	60	[35]
1999	43	[35]
2000	56	[35]
2001	59	[35]
2002	87	[36]
2003	69	[36]
2004	55	[36]
2005	95	[36]
2006	80	[36]
2007	70	[36]
2008	135	[36]
2009	140	[36]
2010	210	[36]
2011	320	[36]
2012	364	[37]
2013	314	[38]
2014	493	[39]
2015	510	[40]
2016	415	[41]
2017	291	[42]
2018	475	[43]
2019	599	[44]
2020	542	[45]
2021	715	[46]
2022	282	[47]
2023	622	[48]

According to the WHO and Moroccan Ministry of health (Table 2), we use the report of malaria case data in Morocco from 1990 to 2023 to estimate the parameters of the model systems (2.1)–(2.6). $S_0 = 50{,}000$, $A_0 = 100$, $I_0 = 110$, $R_0 = 0$, $S_{V_0} = 1000$, and $I_{V_0} = 50$ are the initial conditions chosen

for the human and vector compartments based on contextual data from the same time period. To estimate the difference between declared and simulated human infection cases, we based the analysis on previous research to take the values of confidence intervals of some parameters [49, 50] , and others are assumed; these assumptions are linked to the official national context, which makes them scientifically justified [51]. The rest of the parameters are determined via the following: (i) the least-squares data fitting method [52], to achieve the best possible fitting between the data declared in Morocco and systems (2.1)–(2.6), (ii) the Extended Kalman Filter (EKF). which allows for a joint state-parameter estimation in the presence of nonlinear dynamics; and (iii) a LSTM deep learning model directly trained on historical malaria case data.

6.1. Least squares method

Table 1 describes the values for all the parameters fitted or assumed, and Figure 3 shows the fitted curve of the incidence of malaria in Morocco.

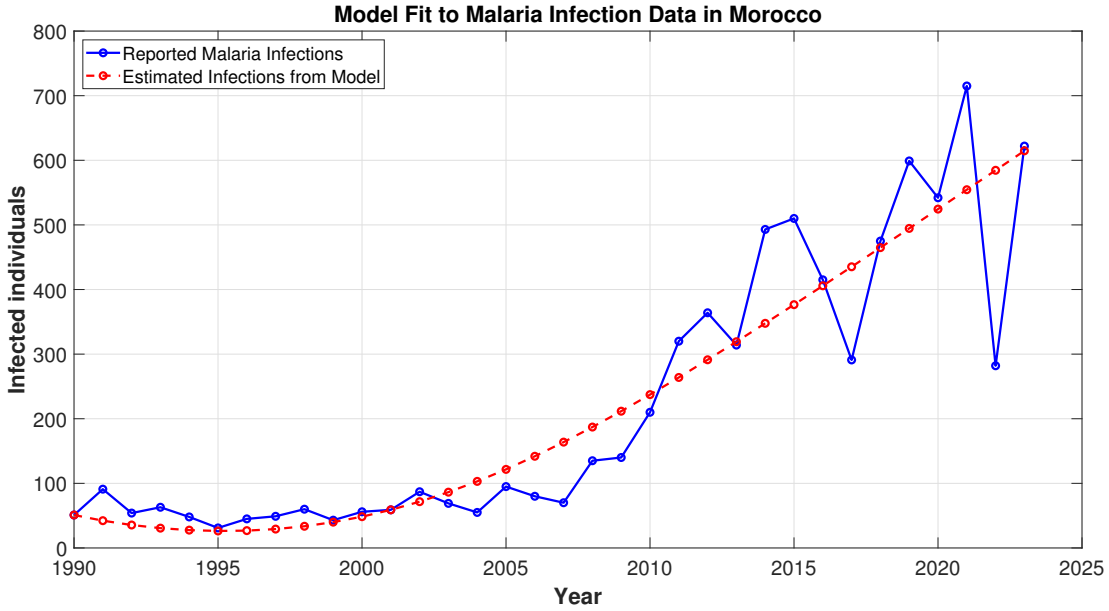

Figure 3. Fitting the imported individuals infected by malaria to its real data in Morocco from 1990 to 2023.

6.2. Extended Kalman Filter (EKF)

An EKF is useful for the estimation of nonlinear dynamical systems [53, 54]. Here, we treat the imported malaria case counts as a second-order latent process s follows:

$$\mathbf{x}_t = \mathbf{F}_t \mathbf{x}_{t-1} + \mathbf{w}_t, \qquad \mathbf{F}_t = \begin{bmatrix} 1 & \Delta t \\ 0 & 1 \end{bmatrix}, \tag{6.1}$$

$$\mathbf{z}_t = \mathbf{H}_t \mathbf{x}_t + \mathbf{v}_t, \qquad \mathbf{H}_t = \begin{bmatrix} 1 & 0 \end{bmatrix}, \tag{6.2}$$

where $\mathbf{x}_t = \begin{bmatrix} y_t & \dot{y}_t \end{bmatrix}^\top$ is some hidden state vector, with y_t being the case count and $\dot{y}_t$ being the rate

of change. The process noise $\mathbf{w}_t \sim \mathcal{N}(0, \mathbf{Q})$ and observation noise $\mathbf{v}_t \sim \mathcal{N}(0, \mathbf{R})$ are assumed to be zero-mean Gaussian noises with covariance matrices that are tuned:

$$\mathbf{Q} = \begin{bmatrix} 2.0 & 0 \\ 0 & 0.1 \end{bmatrix}, \qquad \mathbf{R} = [4]. \tag{6.3}$$

The recursive filter alternates between prediction and correction steps to estimate the latent trajectory $\mathbf{x}_t$ over time.

6.3. Long Short-Term Memory (LSTM)

LSTM is a type of recurrent neural network (RNN) that synthesizes long-range temporal dependencies through gating mechanisms [55, 56]. Operations in an LSTM unit proceed as follows:

$$\begin{aligned}
f_t &= \sigma(W_f[h_{t-1}, x_t] + b_f) && \text{(forget gate)},\\
i_t &= \sigma(W_i[h_{t-1}, x_t] + b_i) && \text{(input gate)},\\
\tilde{C}_t &= \tanh(W_C[h_{t-1}, x_t] + b_C) && \text{(cell update)},\\
C_t &= f_t \odot C_{t-1} + i_t \odot \tilde{C}_t && \text{(cell state)},\\
o_t &= \sigma(W_o[h_{t-1}, x_t] + b_o) && \text{(output gate)},\\
h_t &= o_t \odot \tanh(C_t) && \text{(hidden state)},
\end{aligned}$$

In this expression, σ denotes the sigmoid activation, while $\odot$ refers to element-wise multiplication. Two LSTM layers feature in the module, containing 256 and 64 hidden units, respectively, and dropout regularization ($p = 0.2$). The input memory amounts to $n_{\text{input}} = 5$ years. The Adam optimizer and mean squared error loss are used in its deployment.

6.4. Extended Kalman Filter: Joint state and parameter estimation

To specify the provided malaria case data with the mechanistic transmission model, a reduced host-vector system whose state is given by a nonlinear state–space representation. Now, the EKF is considered to be a joint state–parameter estimator, by means of which the epidemiological compartments and important biological parameters are updated sequentially in time whenever new data appear. A schematic overview of the EKF workflow is given by Figure 4.

Augmented State Vector. We augment the six compartmental states of the reduced malaria model,

$$X_t^{(s)} = (S_t, A_t, I_t, R_t, S_{V,t}, I_{V,t})^\top, \tag{6.4}$$

with a ten-dimensional parameter vector

$$\phi = (d_S, d_A, d_I, d_R, d_V, \beta_1, \beta_2, \gamma, \theta, \varepsilon)^\top, \tag{6.5}$$

taken as time-invariant but unknown.
Therefore, the complete EKF state vector is as follows:

$$X_t = (X_t^{(s)}, \phi)^\top \in \mathbb{R}^{16}. \tag{6.6}$$

Process Model. The continuous-time dynamics of the reduced host-vector system are given by the following:

$$\begin{aligned}
\dot{S} &= \Lambda_S - d_S S - \beta_1 S I_V, \\
\dot{A} &= \Lambda_A - (d_A + \theta) A + \varepsilon \beta_1 S I_V, \\
\dot{I} &= (1-\varepsilon)\beta_1 S I_V + \theta A - (\gamma + d_I + \alpha) I, \\
\dot{R} &= \Lambda_R - d_R R + \gamma I, \\
\dot{S}_V &= \Lambda_V - \beta_2 S_V (A + \kappa I) - d_V S_V, \\
\dot{I}_V &= \beta_2 S_V (A + \kappa I) - d_V I_V.
\end{aligned}$$

From these, the parameter vector satisfies

$$\dot{\phi} = 0,$$

that is, a prior for the random-walk parameter.

Utilizing an Euler discretization with the step size $\Delta t = 1$ year, we obtain a discrete-time process equation in the following form:

$$X_{t+1} = f(X_t) + w_t, \tag{6.7}$$

where $f(\cdot)$ stacks one-step updates of the six compartments and keeps ϕ unchanged.

The noise term $w_t \sim \mathcal{N}(0, Q)$ accounts for model uncertainty, unobserved variability, and seasonal variations model nonrepresentation.

Observation Model. Only the infected human compartment I_t is observed, thus corresponding to the reported annual malaria cases:

$$z_t = h(X_t) + v_t = I_t + v_t, \tag{6.8}$$

where $v_t \sim \mathcal{N}(0, R)$ denotes the measurement noise. Consequently, the Jacobian of the measurement function is as follows:

$$H_t = \frac{\partial h}{\partial X_t} = (0, 0, 1, 0, 0, 0, 0, \ldots, 0), \tag{6.9}$$

with the third component of the state vector being selected.

EKF Prediction and Update. At year t for each time step, the EKF does the following at year end:

1) **Prediction:** propagate the previous state through the nonlinear model:

$$X_{t+1}^{-} = f(X_t), \qquad P_{t+1}^{-} = F_t P_t F_t^{\top} + Q, \tag{6.10}$$

where $F_t = \frac{\partial f}{\partial X_t}$ is the Jacobian of the process model.

2) **Correction:** Update the state prediction based on observed malaria cases:

$$K_t = P_{t+1}^{-} H_t^{\top} (H_t P_{t+1}^{-} H_t^{\top} + R)^{-1}, \tag{6.11}$$

$$X_{t+1} = X_{t+1}^{-} + K_t \left(z_t - h(X_{t+1}^{-}) \right), \qquad P_{t+1} = (I - K_t H_t) P_{t+1}^{-}. \tag{6.12}$$

From Figure 4 below, it is evident that the quantity $z_t - h(X_{t+1}^-)$ scatters through the Kalman gain over the entire 16-dimensional state vector, meaning that the EKF's update impacts both the volumes and the parameters ϕ.

Table 1 shows the values of the EKF-estimated parameters from the posterior mean of ϕ at the end of 2023.

Outputs. The following results are obtained by the EKF:

- An I_t time series estimate of humans infected with malaria that is almost in line with the data;
- Yearly guesses of the parameters associated with the pathogen $\ldots (d_S, d_A, d_I, d_R, d_V, \beta_1, \beta_2, \gamma, \theta, \varepsilon)$.

This approach constructs a theoretically grounded statistical bridge between the mechanistic model and the observed malaria data.

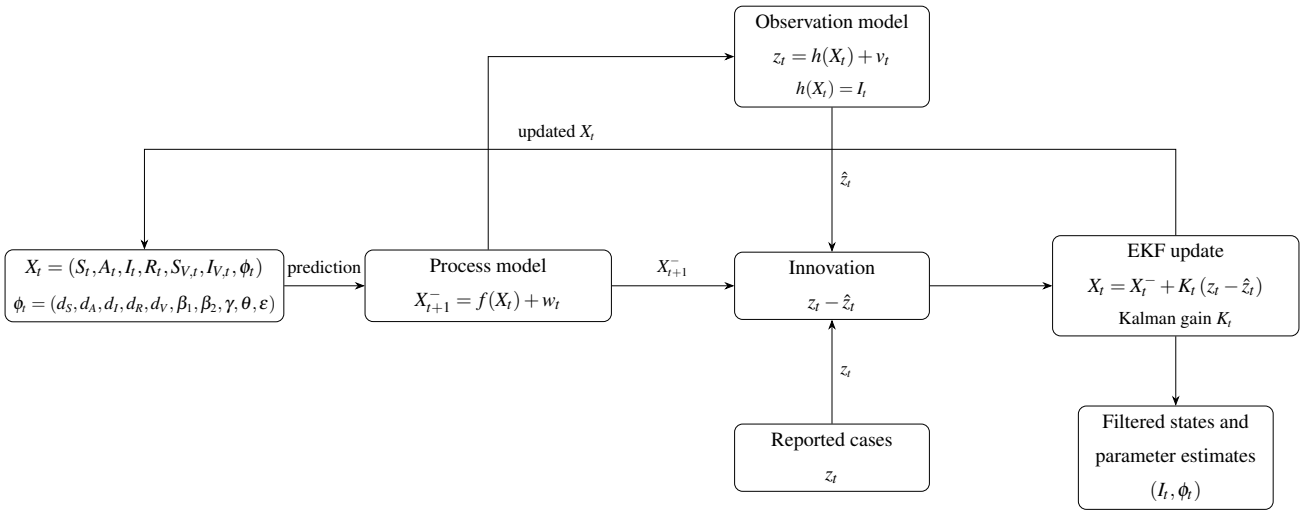

Figure 4. EKF workflow for the malaria model. The filter updates both the compartment states and the epidemiological parameters using reported infections.

6.5. Evaluation metrics

We measure the forecasting skill on historical data (1990–2023) by considering the following three standard metrics:

Mean squared error (MSE):

$$\mathrm{MSE} = \frac{1}{N}\sum_{t=1}^{N}(y_t - \hat{y}_t)^2. \tag{6.13}$$

Mean absolute error (MAE):

$$\text{MAE} = \frac{1}{N}\sum_{t=1}^{N}|y_t - \hat{y}_t|. \tag{6.14}$$

Coefficient of determination (R^2):

$$R^2 = 1 - \frac{\sum_{t=1}^{N}(y_t - \hat{y}_t)^2}{\sum_{t=1}^{N}(y_t - \bar{y})^2}. \tag{6.15}$$

The metrics are computed with the observed malaria cases y_t, predicted values $\hat{y}_t$, and the sample mean $\bar{y}$ over N time points.

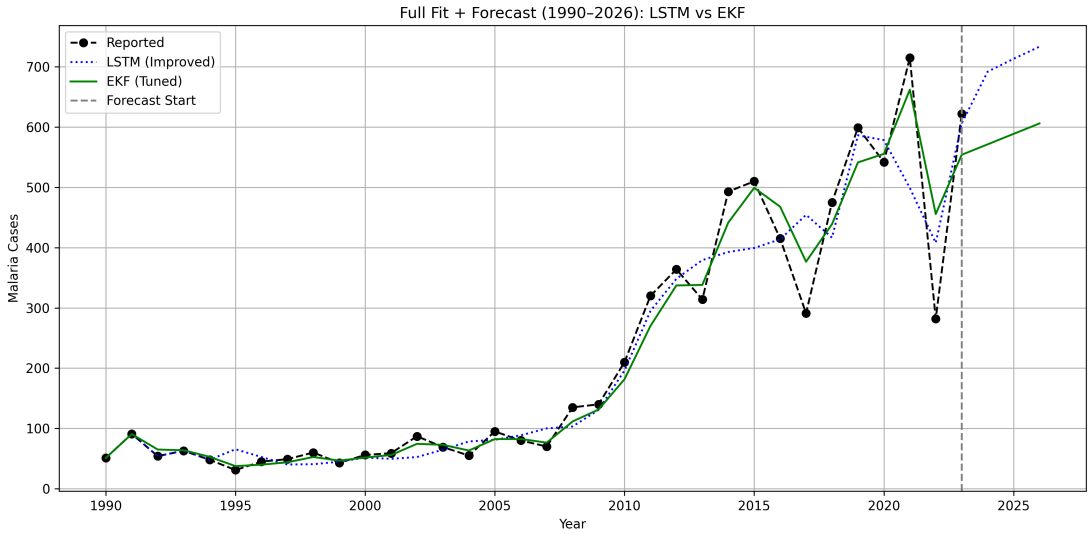

Figure 5. EKF and LSTM model fit to historical malaria case data in Morocco (1990–2026), including forecast for 2024–2026.

Table 3 and Figure 5 reflect the lower prediction error and higher R^2 measure exhibited by the EKF, meaning that the EKF results in an improved fitting of the observed malaria case data as compared to the LSTM.

Table 3. Model performance comparison for malaria case prediction (1990–2023). EKF outperforms LSTM in all metrics.

Model	MSE	MAE	$\mathbf{R^2}$
LSTM	3759.14	35.362718	0.910964
EKF	1802.911934	25.361958	0.957298

7. Optimal control problem

The primary objective of this paper is to reduce the risk of malaria transmission in the presence of human immigration. To make this, appropriate interventions should be taken to ensure that the

number of both infected populations I and I_V stay low throughout the period from 0 to the final time T. Therefore, we suggested distinct control strategies. For the first strategy, u_1 represents awareness campaigns and takes precautions to reduce the exposure. As we know, awareness alone is not sufficient to limit the transmission of malaria. For that, we introduce the second strategy, where u_2 represents chemoprophylaxis and treatment, which helps reduce the number of infected human individuals I, but the risk of the transmission persists because the existence of the infected vectors makes the transmission exist. For that, we add the third control u_3, which represents the effectiveness of the treatment of the Malaria cases, which are Artemisinin-based Combination Therapies (ACTs) in the case of uncomplicated Plasmodium falciparum malaria or Intravenous (IV) Artesunate in the case of the severe cases. Finally, we consider the effectiveness of insecticides, which is represented by u_4. These controls represent Long-Lasting Insecticidal Nets (LLINs) and Indoor Residual Spraying (IRS). These control measures are introduced in our models (2.1)–(2.6), and this system becomes a new model with control strategies provided by the following :

$$\frac{dS}{dt} = (1-u_1)\Lambda_S - d_S S - (1-u_2)\beta_1 S I_V, \tag{7.1}$$

$$\frac{dA}{dt} = (1-u_1)\Lambda_A - (d_A+\theta)A + \varepsilon(1-u_2)\beta_1 S I_V, \tag{7.2}$$

$$\frac{dI}{dt} = (1-\varepsilon)(1-u_2)\beta_1 S I_V + \theta A - (\gamma + d_I + \alpha + u_3)I, \tag{7.3}$$

$$\frac{dR}{dt} = (1-u_1)\Lambda_R - d_R R + (\gamma+u_3)I, \tag{7.4}$$

$$\frac{dS_V}{dt} = \Lambda_V - (1-u_2)\beta_2 S_V(A+\kappa I) - (d_V+u_4)S_V, \tag{7.5}$$

$$\frac{dI_V}{dt} = (1-u_2)\beta_2 S_V(A+\kappa I) - (d_V+u_4)I_V, \tag{7.6}$$

$$\text{with:} \qquad \big(u_1(t), u_2(t), u_3(t), u_4(t)\big) \in U_{\text{ad}}^T, \tag{7.7}$$

$$U_{\text{ad}}^T = \left\{ u = (u_1(t), u_2(t), u_3(t), u_4(t)) \;\middle|\; \begin{array}{l} (u_1(t), u_2(t), u_3(t), u_4(t)) \text{ are measurable,} \\ 0 \le u_1(t) \le 1,\ 0 \le u_2(t) \le 1, \\ 0 \le u_3(t) \le 1,\ 0 \le u_4(t) \le 1 \ \text{ with } t \in [0,T] \end{array} \right\}. \tag{7.8}$$

7.1. Existence of optimal control

We propose the following cost function J, which we aim to minimize and keep the spread of infection to a minimum in both human people and vectors. J is defined by the following:

$$J(u_1,u_2,u_3,u_4) \;=\; \int_0^T \Big[D_1 I \;+\; D_2 I_V \;+\; \tfrac{1}{2}\Big(B_1 u_1^2 \;+\; B_2 u_2^2 \;+\; B_3 u_3^2 \;+\; B_4 u_4^2 \Big) \Big]\, dt. \tag{7.9}$$

The parameters D_1 and D_2 represent the non-negative weights attributed to human and vector infection levels, respectively, whereas B_1, B_2, B_3, and B_4 are the balance parameters linked to the execution of the controls u_1, u_2, u_3, and u_4, respectively.

We aim to determine the optimal controls $u_1^*, u_2^*, u_3^*, u_4^*$ in the admissible set U_{ad}^T that achieve the following

$$J\left(u_1^*, u_2^*, u_3^*, u_4^*\right) = \min_{(u_1,u_2,u_3,u_4)\in U_{\text{ad}}^T} J\left(u_1, u_2, u_3, u_4\right). \tag{7.10}$$

Theorem 7.1. *Consider the control systems (7.1)–(7.6) and the objective functional $J(u_1,u_2,u_3,u_4)$. There exists an optimal control $\left(u_1^*, u_2^*, u_3^*, u_4^*\right) \in U_{ad}^T$ such that* (7.10).

Proof. To establish the existence of an optimal control, we invoke a standard result [57] to ensure that, under suitable continuity and convexity assumptions, every minimizing sequence in a closed and convex admissible control set has a convergent subsequence whose limit achieves the infimum of the objective functional.

Since all state and control variables remain nonnegative and bounded by construction, the set U_{ad}^T is a closed and convex subset of a suitable normed space. Moreover, our objective functional J is convex in the control variables (due to the quadratic cost terms) and is continuous. Consequently, Filippov's Theorem (or an analogous result from the calculus of variations) guarantees the existence of a control $\left(u_1^*, u_2^*, u_3^*, u_4^*\right)$ that attains the global minimum of J.

7.2. Characterization of the optimal control

The Pontryagin Maximum Principle is used based on the Hamiltonian $H(t)$ to formulate the optimality conditions. $H(t)$ is defined by the following:

$$H(t) = D_1 I + D_2 I_V + \frac{1}{2}(B_1 u_1^2 + B_2 u_2^2 + B_3 u_3^2 + B_4 u_4^2) + \lambda_1 \dot{S} + \lambda_2 \dot{A} + \lambda_3 \dot{I} + \lambda_4 \dot{R} + \lambda_5 \dot{S_V} + \lambda_6 \dot{I_V}. \tag{7.11}$$

Theorem 7.2. *Let $S^*(t), A^*(t), I^*(t), R^*(t), S_V^*(t), I_V^*(t)$ denote the optimal state trajectories that correspond to the optimal control variables $\left(u_1^*(t), u_2^*(t), u_3^*(t), u_4^*(t)\right)$ for the optimal control problems* (7.1)–(7.6). *Then, the adjoint variables $\lambda_1, \lambda_2, \lambda_3, \lambda_4, \lambda_5$, and λ_6 satisfy the following:*

$$\begin{aligned}
\dot{\lambda_1}(t) &= \lambda_1 d_S + (1-u_2)(\lambda_1-\lambda_3)\beta_1 I_V + (1-u_2)\beta_1 I_V \varepsilon(\lambda_3-\lambda_2),\\
\dot{\lambda_2}(t) &= d_A\lambda_2 + \theta(\lambda_2-\lambda_3) + \beta_2 S_V(1-u_2)(\lambda_5-\lambda_6),\\
\dot{\lambda_3}(t) &= -D_1 + \lambda_3(d_I+\alpha) + (\gamma+u_3)(\lambda_3-\lambda_4) + \beta_2 S_V(1-u_2)\kappa(\lambda_5-\lambda_6),\\
\dot{\lambda_4}(t) &= d_R\lambda_4,\\
\dot{\lambda_5}(t) &= \beta_2(1-u_2)(A+\kappa I)(\lambda_5-\lambda_6) + \lambda_5(d_V+u_4),\\
\dot{\lambda_6}(t) &= -D_2 + (1-u_2)\beta_1 S I_V(\lambda_1 - \varepsilon\lambda_2 - (1-\varepsilon)\lambda_3) + \lambda_6(d_V+u_4),
\end{aligned} \tag{7.12}$$

with the following conditions of transversality at the final time:

$$\lambda_1(T) = \lambda_2(T) = \lambda_3(T) = \lambda_4(T) = \lambda_5(T) = 0. \tag{7.13}$$

$$\lambda_3(T) = D_1 \text{ And } \lambda_6(T) = D_2. \tag{7.14}$$

Moreover, the optimal control $(u_1^*, u_2^*, u_3^*, u_4^*)$ is provided by the following

$$\begin{aligned} u_1^* &= \max\left\{\min\left(\frac{\lambda_1\Lambda_S+\lambda_2\Lambda_A}{B_1},1\right),0\right\},\\ u_2^* &= \max\left\{\min\left(\frac{\beta_1 SI_V(\varepsilon\lambda_2+(1-\varepsilon)\lambda_3-\lambda_1)+\beta_2 S_V(A+\kappa I)(\lambda_5-\lambda_6)}{B_2},1\right),0\right\},\\ u_3^* &= \max\left\{\min\left(\frac{I(\lambda_3-\lambda_4)}{B_3},1\right),0\right\},\\ u_4^* &= \max\left\{\min\left(\frac{\lambda_5 S_V+\lambda_6 I_V}{B_4},1\right),0\right\}. \end{aligned} \tag{7.15}$$

8. Numerical simulation

This section presents numerical simulation results that assess the impact of optimal control strategies on malaria transmission dynamics, with and without control interventions. The Runge–Kutta method of order four (RK4) was implemented in MATLAB to numerically solve the system of equations numerically. The simulations were carried out over a period of 35 years using the parameter values estimated from real data, as listed in Table 1. This parameter value setting was obtained by implementing the EKF on the historical malaria case data to simultaneously estimate the hidden epidemiological compartments and the key transmission parameters. EKF was able to provide biologically interpretable time-invariant parameters to maintain consistency between the simulation and the observed trend. The control weights in the objective functional were set as follows: $D_1 = 50$, $D_2 = 20$, $B_1 = 2$, $B_2 = 3$, $B_3 = 1.3534$, and $B_4 = 0.7358$. Figures 6 and 7 illustrate the evolution of the human and vector compartments under both scenarios. The aim was to evaluate the effectiveness of the proposed control measures in reducing the spread of malaria.

The results show that applying optimal control significantly reduces the number of asymptomatic and symptomatic infected human individuals, while increasing the number of recovered individuals. These outcomes confirm the effectiveness of the proposed strategy.

Figures 6 shows the evolution of all human and vectors population compartments respectively under both scenarios with control (blue curves) and without control (red curves).

As illustrated in Figure 6, there is a clear contrast between the scenario without controls and the scenario with controls. Without controls, S sharply decreases , thus reflecting an increase in A and I, though R also increases, albeit modestly. After controls are applied, the dynamics are reversed: S no longer decreases at the same rate and tends to stabilize, A remains broadly stable with a slight decline, while I declines sharply over approximately six years, thus highlighting the effectiveness of the control measures.

Additionally, this change also has an impact on the vector populations, as shown in Figure 7. In the absence of control, infected vectors I_V remain active for nearly 35 years, while susceptible vectors S_V, despite their high numbers, decline because some of them become infected. Once control strategies are implemented, both groups rapidly decline, thus confirming the impact of the interventions.

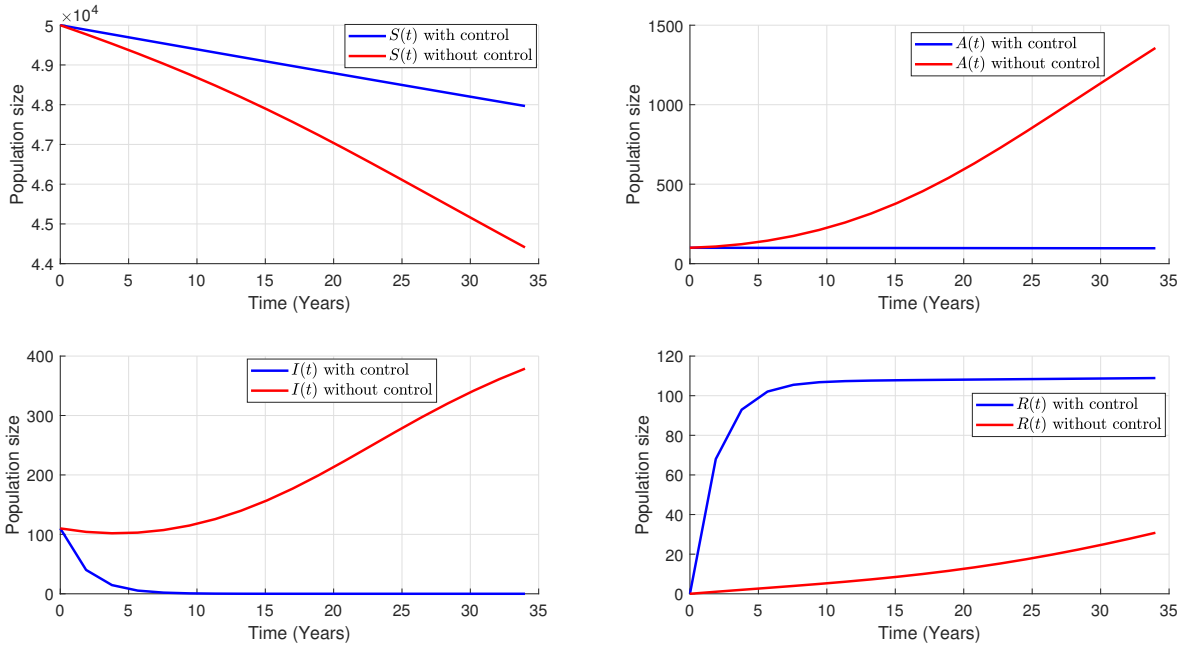

Figure 6. Time series of the state variables S, A, I, and R without and with controls.

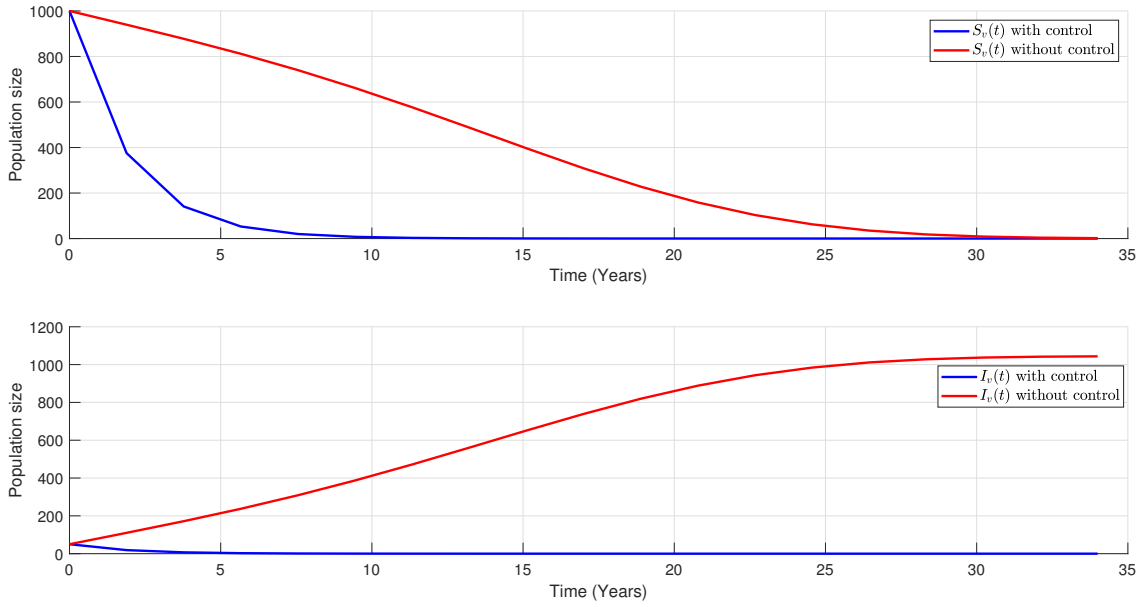

Figure 7. Time series of the state variables S_V and I_V without and with controls.

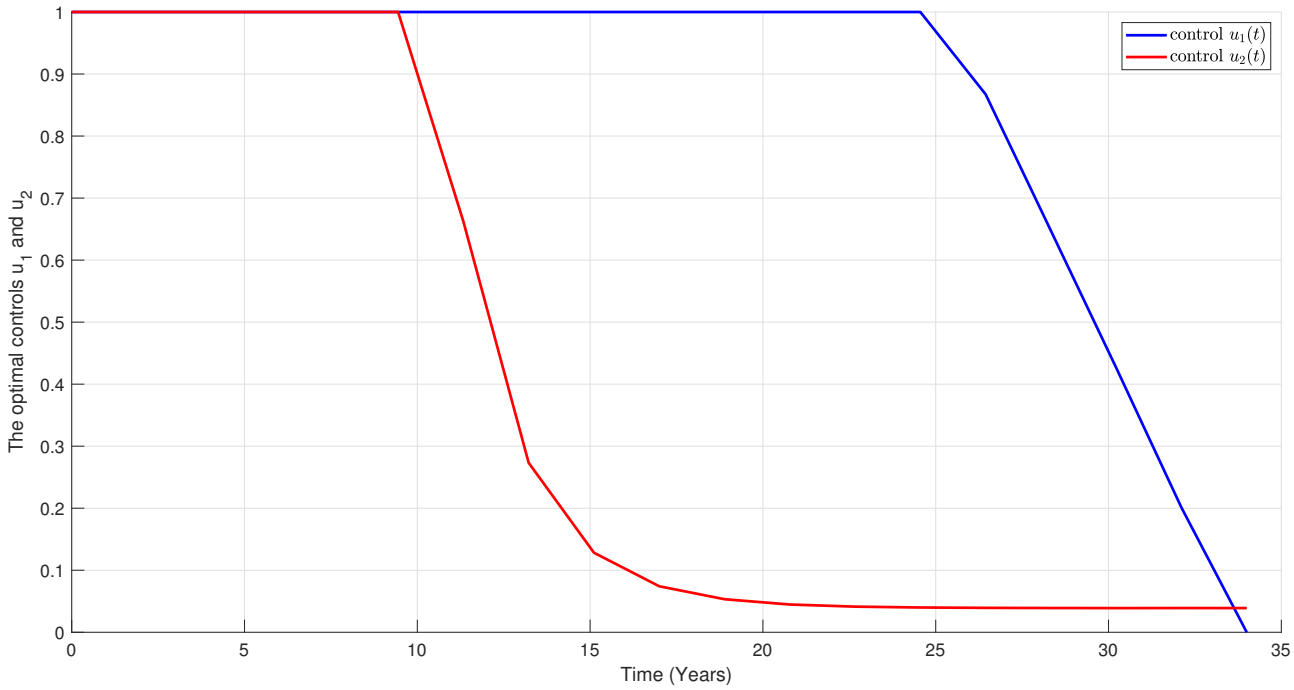

Figure 8. Optimal controls $u_1(t)$ and $u_2(t)$.

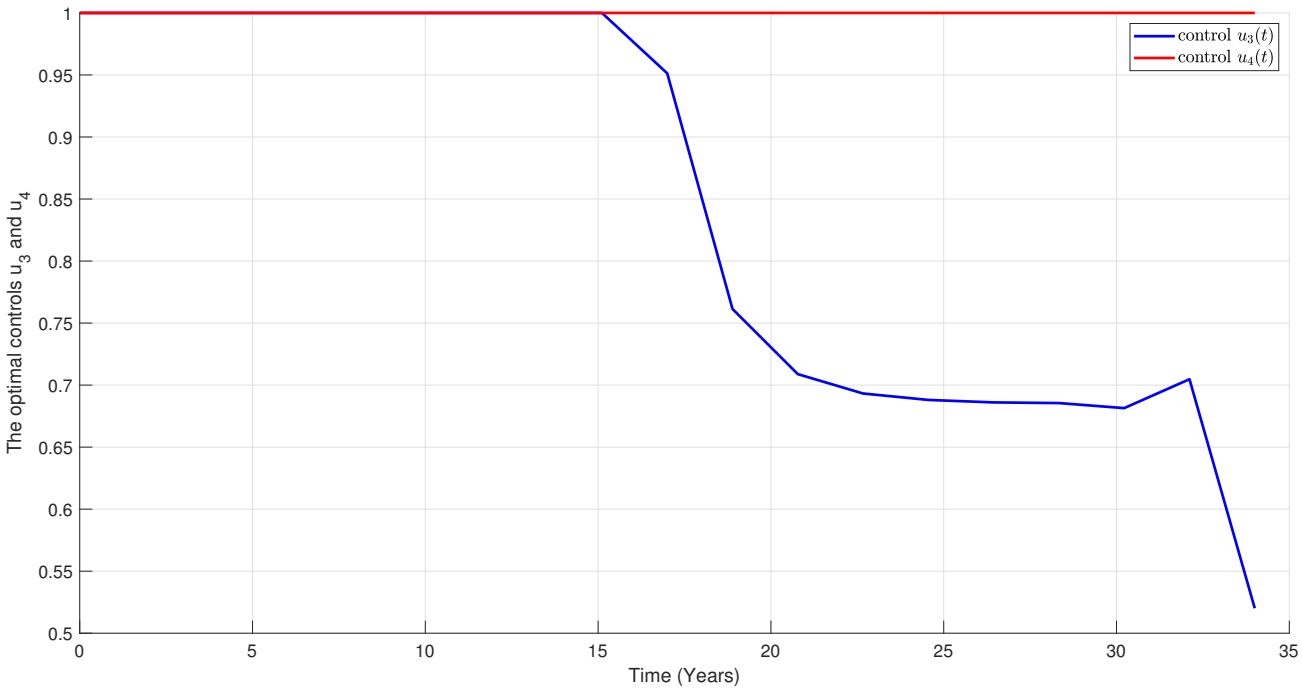

Figure 9. Optimal controls $u_3(t)$ and $u_4(t)$.

In Figures 8 and 9, we see that all controls start at their maximum allowable value of 1, which shows that the initial intervention strategy had an effect. For $u_1(t)$, which stands for vaccination or treatment aimed at the human population, the intensity stays at a full level for 7 years before quickly dropping to about 0. In the same way, $u_3(t)$ follows a path that is almost the same as $u_1(t)$, thereby starting at full intensity and then slowly getting weaker over the course of four years.

9. Conclusions and perspective

Human movement still poses a viable challenge for the ambitious goal of Global Malaria Elimination. The only challenge is well-settled in some parts of the world that are constantly threatened by imported cases. In this study, a deterministically compartmental model was developed,thereby explicitly incorporating human migration in malaria transmission dynamics using Morocco as a representative case study. By combining migration processes in both human and vector populations, the model puts the two processes inside a rigorous framework for to assess the likelihood of reintroducing of malaria in a malaria-free setting.

From a theoretical point of view, the strong positivity, boundedness, and uniqueness of the solution to the model were established. This is because the influx of potentially infected people is never-ending, where the system does not admit a disease-free equilbrium but instead an endemic one, which is unique. Here, we see that this equilibrium point is globally asymptotically stable when given strong analytically verified restrictions, that is, malaria is driven to remain endemic at stable levels when imported and hence unseen transmission when local endemic transmission is switching off. The stress of these endpoints is developmental roles in population movement for the persistence of malaria risk.

In order to link the mathematical model to data from the real world, in Morocco, reported data on malaria cases from 1990 to 2023 were exposed to three parameter estimation methods. The EKF was used to estimate the hidden state elements for epidemiology and some key transmission parameters by joint optimization to the same state-space structure. In parallel, an LSTM neural network was trained on partial case data. The results of the comparison were stark: the EKF structure did exceedingly better compared with other standardized mathematical models in prediction, thus highlighting the very crucial importance of incorporating mechanistic and statistical approaches when modeling imported infectious diseases.

In addition to developing optimal control framework to optimize the exploration of strategies for to minimize malaria transmission in the presence of imported cases, the application of Pontryagin's Maximum Principle illustrated the need for the joint use of various intervention methods such as building public awareness, chemoprophylaxis, treatment, and the use of larvicides, which can lead to a significant reduction in both human and vector-derived infections. From the numerical simulations, it was observed that when such strategies and targeted preventive interventions are carried out at an early stage and are sustained, these imported cases will have a long-term minimum effect.

From a public health perspective, it is imperative to stress that being free of malaria requires an active surveillance policy that takes population movement into consideration. Awareness measures, coupled with the means to limit the influence of vectors, followed by early treatment possibilities, can serve as an effective counter scheme to redefine national malaria control efforts, especially in countries located along the major migration routes.

Beyond the Moroccan context, the proposed framework is versatile and can be adapted to any

location undergoing the same risks for disease due to mobility. Future work may detail the model with stochastic migration movements, climate-modulated changes in vector habitat, and spatial heterogeneity to provide an extensive tool for anticipating and mitigating re-emergence of malaria and other vector-borne illness in high-mobility setting.

Use of Generative-AI Tools Declaration

The authors declare that no artificial intelligence (AI) tools were used in the preparation of this manuscript.

Conflict of interest

The authors declare that they have no conflict of interest in this paper.

Acknowledgements

The authors would like to thank the anonymous reviewers for their valuable comments that help improve the quality of our work. A. Tridane would like to thank the guest editor for their kind invitation to contribute to this special issue in honor of my dear friend and mentor, Prof. Yang Kuang.

Funding

A. Tridane is funded by SQU-UAEU grant 12S243.

References

1. World Health Organization (WHO), World malaria report 2023. Available from: https://www.who.int/teams/global-malaria-programme/reports/world-malaria-report-2023.
2. World Health Organization (WHO), World malaria report 2024. Available from: https://www.who.int/teams/global-malaria-programme/reports/world-malaria-report-2024.
3. Medicines for Malaria Venture, Causes of malaria, 2023. Available from: https://www.mmv.org/malaria/about-malaria/causes-malaria.
4. World Health Organization, Malaria fact sheet, 2023. Available from: https://www.who.int/news-room/fact-sheets/detail/malaria.
5. World Health Organization, Malaria data and statistics, 2023. Available from: https://www.who.int/data/gho/data/themes/malaria.
6. M. Roser, H. Ritchie, Malaria, Our World in Data, 2015. Available from: https://ourworldindata.org/malaria.
7. World Health Organization, Malaria: Questions and answers, World Health Organization, 2023. Available from: https://www.who.int/news-room/questions-and-answers/item/malaria.

8. Medicines for Malaria Venture, Malaria facts and statistics, 2025. Available from: https://www.mmv.org/malaria/about-malaria/malaria-facts-statistics-2025.

9. K. C. Mezieobi, E. U. Alum, O. Paul-Chima Ugwu, D. E. Uti, B. N. Alum, S. I. Egba, et al., Economic burden of malaria on developing countries: A mini review, *Parasite Epidemiol. Control*, **30** (2025), e00435. https://doi.org/10.1016/j.parepi.2025.e00435

10. F. Ricci, Social implications of malaria and their relationships with poverty, *Mediterr. J. Hematol. Infect. Dis.*, **4** (2012), e2012048. https://doi.org/10.4084/MJHID.2012.048

11. G. K. Amina, Socio-economic determinants and malaria risk: Assessing the impact of poverty, housing conditions, and healthcare accessibility in high-incidence regions, *Sciences*, **5** (2024), 120–124. https://doi.org/10.59298/nijrms/2024/5.3.120124

12. World Health Organization, *Global technical strategy for malaria 2016–2030*, World Health Organization, Geneva, 2015. Available from: https://www.who.int/publications/i/item/9789240031357.

13. Centers for Disease Control and Prevention, Strategies for reducing malaria's global impact, April 1, 2024. National Center for Emerging and Zoonotic Infectious Diseases (NCEZID). Available from: https://www.cdc.gov/malaria/php/public-health-strategy/index.html.

14. International Organization for Migration, Malaria and mobility, Information Sheet, Migration Health Division, International Organization for Migration, 24 April 2018. Available from: https://www.iom.int/sites/default/files/our_work/DMM/Migration-Health/mhd_infosheet_malaria_and_mobility_24.04.2018.pdf.

15. European Centre for Disease Prevention and Control, Malaria: Annual epidemiological report for 2022. ECDC Surveillance Report. Available from: https://www.ecdc.europa.eu/en/publications-data/malaria-annual-epidemiological-report-2022.

16. Z. Herrador, B. Fernández-Martinez, V. Quesada-Cubo, O. Diaz-Garcia, R. Cano, A. Benito, et al., Imported cases of malaria in spain: Observational study using nationally reported statistics and surveillance data, 2002–2015, *Malar. J.*, **18** (2019), 230. https://doi.org/10.1186/s12936-019-2863-2

17. K. Nabah, N. Mezzoug, A. Aarab, H. Oufdou, K. Rharrabe, Epidemiological profile of imported malaria in the northern region of Morocco, 2014–2018, *E3S Web Conf.*, **319** (2021), 01057. https://doi.org/10.1051/e3sconf/202131901057

18. A. Hanafi, I. Zouaoui, H. Abjabja, Y. Abercha, S. Aoufi, Imported malaria at the ibn sina university hospital in rabat: A retrospective study of 81 cases, *Cureus*, **16** (2024), e60253. https://doi.org/10.7759/cureus.60253

19. H. El Amouri, Sub-saharan immigration to morocco: Some impacts of human mobility on a state's domestic policy and geopolitics, *Int. Social Sci. Manage. J.*, **2022** (2022).

20. N. W. Ruktanonchai, P. DeLeenheer, A. J. Tatem, V. A. Alegana, T. T. Caughlin, E. zu Erbach-Schoenberg, et al., Identifying malaria transmission foci for elimination using human mobility data, *Comput. Biol.*, **12** (2016), e1004846. https://doi.org/10.1371/journal.pcbi.1004846

21. O. Abdelkrim, Z. Said, L. Souad, Anopheles mosquitoes in Morocco: Implication for public health and underlined challenges for malaria re-establishment prevention under current and future climate conditions, *Pest. Manage. Sci.*, **80** (2024), 2085–2095. https://doi.org/10.1002/ps.7943

22. J. C. Semenza, J. E. Suk, Vector-borne diseases and climate change: A European perspective, *FEMS Microbiol. Lett.*, **365** (2018), fnx244. https://doi.org/10.1093/femsle/fnx244

23. R. Ross, Some a priori pathometric equations, *Proc. R. Soc. London, Ser. A*, **81** (1908), 465–486. https://doi.org/10.1136/bmj.1.2830.546 .

24. G. Macdonald, *The Epidemiology and Control of Malaria*, Oxford University Press, 1957.

25. K. Dietz, L. Molineaux, A. Thomas, A malaria model tested in the african savannah, *Bull. World Health Organ.*, **50** (1974), 347–357.

26. A. I. Abioye, M. O. Ibrahim, O. J. Peter, H. A. Ogunseye, Optimal control on a mathematical model of malaria, *Sci. Bull., Series A: Appl. Math. Phy.*, **83** (2020), 177–190.

27. G. Otieno, J. K. Koske, J. M. Mutiso, Transmission dynamics and optimal control of malaria in kenya, *Discrete Dyn. Nat. Soc.*, **2016** (2016), 8013574. https://doi.org/10.1155/2016/8013574

28. S. Kim, A. Tridane, D. E. Chang, Human migrations and mosquito-borne diseases in Africa, *Math. Popul. Stud.*, **23** (2016), 123–146. https://doi.org/10.1080/08898480.2015.1054221

29. S. Yacheur, A. Moussaoui, A. Tridane, Modeling the imported malaria to north africa and the absorption effect of the immigrants, *Math. Biosci. Eng.*, **16** (2019), 967–989. https://doi.org/10.3934/mbe.2019045 .

30. A. Rajnarayanan, M. Kumar, A. Tridane, Analysis of a mathematical model for malaria using data-driven approach, *Sci. Rep.*, **15** (2025), 27272. https://doi.org/10.1038/s41598-025-12078-4

31. S. Olaniyi, K. O. Okosun, S. O. Adesanya, R. S. Lebelo, Modelling malaria dynamics with partial immunity and protected travellers: Optimal control and cost-effectiveness analysis, *J. Biol. Dyn.*, **14** (2020), 90–115. https://doi.org/10.1080/17513758.2020.1722265

32. K. Y. Ng, M. M. Gui, COVID-19: Development of a robust mathematical model and simulation package with consideration for ageing population and time delay for control action and resusceptibility, *Physica D: Nonlinear Phenom.*, **411** (2020), 132599. https://doi.org/10.1016/j.physd.2020.132599

33. United Nations Department of Economic and Social Affairs, Population Division, International migrant stock 2024 by sex and destination, 2024. Available from: https://www.un.org/development/desa/pd/content/international-migrant-stock.

34. Macrotrends LLC, Morocco immigration statistics — historical chart & data, 2025. Includes data points for 2000, 2005, 2010, and 2015. Available from: https://www.macrotrends.net/countries/MAR/morocco/immigration-statistics.

35. Ministry of Health of Morocco, National statistics on malaria, 1990–2001. Archived statistical data, 2002. Available through annual statistical reports of the Ministry of Health, Rabat. Available from: https://www.sante.gov.ma.

36. World Health Organization Regional Office for the Eastern Mediterranean, Morocco: Malaria burden and elimination status, 2011. Available from: https://www.emro.who.int/mor/morocco-news/morocco-certified-malaria-free.html.

37. Ministry of Health of Morocco, Health in figures 2012–2013 edition (revised version), 2013. Available from: https://www.sante.gov.ma/Publications/Etudes_enquete.

38. Ministry of Health of Morocco, Health in figures 2013–2014 edition (revised version), 2014. Available from: https://www.sante.gov.ma/Publications/Etudes_enquete.

39. Ministry of Health of Morocco, Health in figures 2014–2015 edition, 2015. Available from: https://www.sante.gov.ma/Publications/Etudes_enquete.

40. Ministry of Health of Morocco, Health in figures 2015–2016 edition, 2016. Available from: https://www.sante.gov.ma/Publications/Etudes_enquete.

41. Ministry of Health of Morocco, Health in figures 2016, 2017. Available from: https://www.sante.gov.ma/Publications/Etudes_enquete.

42. Ministry of Health of Morocco, Health in figures 2017, 2018. Available from: https://www.sante.gov.ma/Publications/Etudes_enquete.

43. Ministry of Health of Morocco, Health in figures 2018, 2019. Available from: https://www.sante.gov.ma/Publications/Etudes_enquete.

44. Ministry of Health of Morocco, Health in figures 2019, 2020. Available from: https://www.sante.gov.ma/Publications/Etudes_enquete.

45. Ministry of Health and Social Protection of Morocco, Health in figures 2020, final version, 2021. Available from: https://www.sante.gov.ma/Publications/Etudes_enquete.

46. Ministry of Health and Social Protection of Morocco, Health in figures 2021, final version, 2024. Available from: https://www.sante.gov.ma/Publications/Etudes_enquete.

47. Ministry of Health and Social Protection of Morocco, Health in figures 2022, final version, 2024. Available from: https://www.sante.gov.ma/Publications/Etudes_enquete.

48. Ministry of Health and Social Protection of Morocco, Health in figures 2023, final version, 2025. Available from: https://www.sante.gov.ma/Publications/Etudes_enquete.

49. N. Chitnis, J. M. Hyman, J. M. Cushing, Determining important parameters in the spread of malaria through the sensitivity analysis of a mathematical model, *Bull. Math. Biol.*, **70** (2008), 1272–1296. https://doi.org/10.1007/s11538-008-9299-0

50. C. Chiziba, S. Silal, Exploring measures to increase detection of malaria cases through reactive case detection in a southern province of zambia-like setup: A modelling study, medRxiv. https://doi.org/10.1101/2024.07.18.24310660

51. Hespress English, Health minister urges stronger malaria prevention among travelers as cases note increase, 2025.

52. E. W. Weisstein, Least squares fitting, MathWorld—A Wolfram Web Resource, Accessed 2022-01-15.

53. A. H. Jazwinski, *Stochastic Processes and Filtering Theory*, Academic Press, New York, 1970.

54. P. S. Maybeck, *Stochastic Models, Estimation, and Control*, Academic Press, New York, 1982.

55. S. Hochreiter, J. Schmidhuber, Long short-term memory, *Neural Comput.*, **9** (1997), 1735–1780. https://doi.org/10.1162/neco.1997.9.8.1735 .

56. K. Greff, R. K. Srivastava, J. Koutník, B. R. Steunebrink, J. Schmidhuber, Lstm: A search space odyssey, *IEEE Trans. Neural Networks Learn. Syst.*, **28** (2017), 2222–2232. https://doi.org/10.1109/TNNLS.2016.2582924

57. W. H. Fleming, R. W. Rishel, *Deterministic and Stochastic Optimal Control*, Springer-Verlag, Berlin, Heidelberg, 1975.

58. G. Birkhoff, G. C. Rota. *Ordinary Differential Equations*, Introductions to Higher Mathematics, Wiley, 1978.

59. H. Toufga, A. Sakkoum, L. Benahmadi, M. Lhous, Analysis of the dynamics and optimal control of cutaneous Leishmania during human immigration, *Iran. J. Numer. Anal. Optim.*, **15** (2025), 311–345. https://doi.org/15(1):311–345, 2025 .

60. J. P. LaSalle, Stability theory for ordinary differential equations, *J. Differ. Equ.*, **4** (1968), 57–65.

Appendix

A. Proof of Theorem 3.1

Proof. We demonstrate that all state variables of systems described by Eqs (2.1)–(2.6) stay non-negative for all $t \geq 0$, provided non-negative initial conditions.

From Eq (2.1),

$$\dot{S}(t) = \Lambda_s - d_S S(t) - \beta_1 S(t) I_v(t) \geq -\big(d_S + \beta_1 I_v(t)\big) S(t). \tag{A.1}$$

This implies the following:

$$\dot{S}(t) + F(t) S(t) \quad \geq \quad 0, \tag{A.2}$$

where $F(t) = d_S + \beta_1 I_v(t)$.

Multiplying both sides by the integrating factor $e^{\int_0^t F(s)\,ds}$, we obtain the following:

$$\frac{d}{dt}\left(S(t)\, e^{\int_0^t F(s)\,ds} \right) \geq 0. \tag{A.3}$$

Integrating from 0 to t yields

$$S(t)\, e^{\int_0^t F(s)\,ds} \geq S(0), \tag{A.4}$$

and hence

$$S(t) \geq S(0)\, e^{-\int_0^t F(s)\,ds} \geq 0. \tag{A.5}$$

By applying similar arguments to Eqs (2.1)–(2.6), we conclude that

$$A(t), I(t), R(t), S_V(t), I_V(t) \geq 0 \text{ for all } t \geq 0.$$

B. Proof of Theorem 3.2

Proof. Systems (2.1)–(2.6) can be written in the following form:

$$\rho(X) = AX + B(X),$$

where X and $\rho(X)$ are defined by the following:

$$X = \begin{bmatrix} S(t) \\ A(t) \\ I(t) \\ R(t) \\ S_V(t) \\ I_V(t) \end{bmatrix} \quad \text{and} \quad \rho(X) = \begin{bmatrix} \dot{S}(t) \\ \dot{A}(t) \\ \dot{I}(t) \\ \dot{R}(t) \\ \dot{S_V}(t) \\ \dot{I_V}(t) \end{bmatrix}.$$

Matrix A and the nonlinear vector $B(X)$ are given by the following:

$$\mathbf{A} = \begin{bmatrix} -d_S & 0 & 0 & 0 & 0 & 0 \\ 0 & -(d_A+\theta) & 0 & 0 & 0 & 0 \\ 0 & \theta & -(\gamma+d_I+\alpha) & 0 & 0 & 0 \\ 0 & 0 & \gamma & -d_R & 0 & 0 \\ 0 & 0 & 0 & 0 & -d_V & 0 \\ 0 & 0 & 0 & 0 & 0 & -d_V \end{bmatrix} \quad \text{and} \quad B(X) = \begin{bmatrix} \Lambda_S - \beta_1 S I_V \\ \Lambda_A + \varepsilon\beta_1 S I_V \\ (1-\varepsilon)\beta_1 S I_V \\ 0 \\ -\beta_2 S_V(A+\kappa I) + \Lambda_V \\ \beta_2 S_V(A+\kappa I) \end{bmatrix}.$$

Let X_1 and X_2 be two arbitrary vectors. Then,

$$B(X_1) - B(X_2) = \begin{bmatrix} -\beta_1 S_1 I_{V_1} + \beta_1 S_2 I_{V_2} \\ \varepsilon\beta_1 S_1 I_{V_1} - \varepsilon\beta_1 S_2 I_{V_2} \\ (1-\varepsilon)\beta_1 S_1 I_{V1} - (1-\varepsilon)\beta_1 S_2 I_{V2} \\ 0 \\ -\beta_2 S_{V_1}(A_1+\kappa I_1) + \beta_2 S_{V_2}(A_2+\kappa I_2) \\ \beta_2 S_{V_1}(A_1+\kappa I_1) - \beta_2 S_{V_2}(A_2+\kappa I_2) \end{bmatrix}.$$

Using the triangle inequality, we obtain the following:

$$\begin{aligned}
\big|B(X_1)-B(X_2)\big| &\le \beta_1\Big|S_2I_{V_2}-S_1I_{V_1}\Big|+\varepsilon\beta_1\Big|S_1I_{V_1}-S_2I_{V_2}\Big|+(1-\varepsilon)\beta_1\Big|S_1I_{V_1}-S_2I_{V_2}\Big|\\
&\quad+\beta_2\Big|S_{V_1}A_1-S_{V_2}A_2\Big|+\kappa\beta_2\Big|S_{V_1}I_1-S_{V_2}I_2\Big|\\
&\le \beta_1\Big(\,|S_2|\,|I_{V_2}-I_{V_1}|+|I_{V_1}|\,|S_2-S_1|\,\Big)\\
&\quad+\varepsilon\beta_1\Big(\,|S_1|\,|I_{V_1}-I_{V_2}|+|I_{V_2}|\,|S_1-S_2|\,\Big)\\
&\quad+(1-\varepsilon)\beta_1\Big(\,|S_1|\,|I_{V_1}-I_{V_2}|+|I_{V_2}|\,|S_1-S_2|\,\Big)\\
&\quad+\beta_2\Big(\,|S_{V_1}|\,|A_1-A_2|+|A_2|\,|S_{V_1}-S_{V_2}|\,\Big)\\
&\quad+\kappa\beta_2\Big(\,|S_{V_1}|\,|I_1-I_2|+|I_2|\,|S_{V_1}-S_{V_2}|\,\Big)\\
&\le M_1\big(|I_{V_1}-I_{V_2}|+|S_1-S_2|\big)+M_2\big(|I_{V_1}-I_{V_2}|+|S_1-S_2|\big)\\
&\quad+M_3\big(|I_{V_1}-I_{V_2}|+|S_1-S_2|\big)+2M_4|A_1-A_2|+2M_5|I_1-I_2|+2M_6|S_{V_1}-S_{V_2}|\\
&\le M\,\|X_1-X_2\|,
\end{aligned}\tag{B.1}$$

where

$$M=\max\{M_1+M_2+M_3,\,2M_4,\,2M_5,\,2M_6\}.$$

The constants M_i, for $i=\{1,\dots,6\}$, are defined by the following

$$\begin{aligned}
M_1&=\beta_1(S^\star+I_V^\star),\\
M_2&=\varepsilon\beta_1(S^\star+I_V^\star),\\
M_3&=(1-\varepsilon)\beta_1(S^\star+I_V^\star),\\
M_4&=\tfrac{1}{2}\beta_2S_V^\star,\\
M_5&=\tfrac{1}{2}\kappa\beta_2S_V^\star,\\
M_6&=\tfrac{1}{2}\beta_2(A^\star+\kappa I^\star),
\end{aligned}\tag{B.2}$$

where

$$\begin{aligned}
S^\star&=\max_{0\le t\le T}S(t),\quad A^\star=\max_{0\le t\le T}A(t),\quad I^\star=\max_{0\le t\le T}I(t),\\
R^\star&=\max_{0\le t\le T}R(t),\quad S_V^\star=\max_{0\le t\le T}S_V(t),\quad I_V^\star=\max_{0\le t\le T}I_V(t).
\end{aligned}\tag{B.3}$$

Consequently, we have the following

$$|\rho(X_1)-\rho(X_2)|\le\mathscr{G}\,|X_1-X_2|,$$

where $\mathscr{G}=\max\{M,\|A\|\}<\infty$. Hence, the function $\rho(X)$ is uniformly Lipschitz continuous.

Moreover, by imposing the non-negativity conditions

$$S(t)\ge 0,\quad A(t)\ge 0,\quad I(t)\ge 0,\quad R(t)\ge 0,\quad S_V(t)\ge 0,\quad I_V(t)\ge 0,$$

the existence of a solution for the systems (2.1)–(2.6) is guaranteed (see [58]).

C. Proof of Theorem 3.3

Proof. Let $N(t)$ denote the total human population and $N_V(t)$ the total vector population, which are defined as follows:

$$\begin{aligned} N(t) &= S(t)+A(t)+I(t)+R(t),\\ N_V(t) &= S_V(t)+I_V(t). \end{aligned}$$

By summing the first four equations of the systems (2.1)–(2.6), we obtain the following:

$$\begin{aligned} \dot{N}(t) &= \dot{S}(t)+\dot{A}(t)+\dot{I}(t)+\dot{R}(t)\\ &= \Lambda_S+\Lambda_A-d_S S-d_A A-d_I I-d_R R-\alpha I\\ &\leq \Lambda_S+\Lambda_A-d_S S-d_A A-d_I I-d_R R\\ &\leq \Lambda_S+\Lambda_A-\max\{d_S,d_A,d_I,d_R\}\,(S+A+I+R)\\ &\leq \Lambda_S+\Lambda_A-\zeta N(t), \end{aligned}$$

where

$$\zeta = \max\{d_S,d_A,d_I,d_R\}$$

denotes the maximum of the natural death rates of the human compartments.

It follows that

$$\limsup_{t\to+\infty} N(t) \leq \frac{\Lambda_S+\Lambda_A}{\zeta},$$

and consequently,

$$N(t) \longrightarrow \frac{\Lambda_S+\Lambda_A}{\zeta} \quad \text{as } t\to+\infty.$$

Similarly, summing the last two equations of systems (2.1)–(2.6) yields the following

$$N_V(t) \longrightarrow \frac{\Lambda_V}{d_V} \quad \text{as } t\to+\infty.$$

D. Proof of Theorem 4.1

Proof. We investigate the existence of an endemic equilibrium for systems (2.1)–(2.6). Let

$$E^* = \left(S^*,A^*,I^*,R^*,S_V^*,I_V^*\right)$$

denote an endemic equilibrium of the model.

To determine this equilibrium, we set the right-hand sides of systems (2.1)–(2.6) equal to zero, which yields the following

$$\Lambda_S - d_S S - \beta_1 S I_V = 0, \tag{D.1}$$

$$\Lambda_A - (d_A+\theta)A + \varepsilon\beta_1 S I_V = 0, \tag{D.2}$$

$$(1-\varepsilon)\beta_1 SI_V + \theta A - (\gamma + d_I + \alpha) I = 0, \tag{D.3}$$

$$\Lambda_R - d_R R + \gamma I = 0, \tag{D.4}$$

$$\Lambda_V - \beta_2 S_V (A + \kappa I) - d_V S_V = 0, \tag{D.5}$$

$$\beta_2 S_V (A + \kappa I) - d_V I_V = 0. \tag{D.6}$$

Solving Eqs (D.1)–(D.5), the equilibrium values of all compartments can be expressed in terms of I_V^* as follows:

$$S^* = \frac{\Lambda_S}{d_S + \beta_1 I_V^*}, \tag{D.7}$$

$$A^* = \frac{1}{d_A + \theta}\left(\Lambda_A + \frac{\varepsilon\beta_1 \Lambda_S I_V^*}{d_S + \beta_1 I_V^*}\right), \tag{D.8}$$

$$I^* = \frac{\Lambda_A \theta (d_S + \beta_1 I_V^*) + \theta\varepsilon\beta_1 \Lambda_S I_V^*}{(\gamma + d_I + \alpha)(d_A + \theta)(d_S + \beta_1 I_V^*)}, \tag{D.9}$$

$$R^* = \frac{\Lambda_R}{d_R} + \frac{\gamma}{d_R}\frac{\Lambda_A \theta (d_S + \beta_1 I_V^*) + \theta\varepsilon\beta_1 \Lambda_S I_V^*}{(\gamma + d_I + \alpha)(d_A + \theta)(d_S + \beta_1 I_V^*)}. \tag{D.10}$$

Moreover,

$$S_V^* = \frac{(\gamma+d_I+\alpha)(d_A+\theta)(d_S+\beta_1 I_V^*)}{\beta_2\Lambda_A(\gamma+d_I+\alpha)(d_S+\beta_1 I_V^*)+\beta_2\varepsilon\beta_1\Lambda_S I_V^*(\gamma+d_I+\alpha)+\beta_2\kappa\Lambda_A\theta(d_S+\beta_1 I_V^*)+\beta_2\kappa\theta\varepsilon\beta_1\Lambda_S I_V^*+d_V(\gamma+d_I+\alpha)(d_A+\theta)(d_S+\beta_1 I_V^*)}.$$

Substituting these expressions into Eq (D.6) yields a quadratic equation in the single unknown I_V^*:

$$\mathscr{A}_1 (I_V^*)^2 + \mathscr{A}_2 I_V^* + \mathscr{A}_3 = 0,$$

where the coefficients are defined by the following:

$$\begin{aligned}
\mathscr{A}_1 &= \beta_1 d_V \beta_2 \Lambda_A (\gamma + d_I + \alpha) + \beta_1 d_V \beta_2 \kappa \Lambda_A \theta + d_V^2 (\gamma + d_I + \alpha)(d_A + \theta)\beta_1 \\
&\quad + d_V \beta_2 \varepsilon \beta_1 \Lambda_S (\gamma + d_I + \alpha) + \beta_2 \kappa \Lambda_A \theta d_V, \\
\mathscr{A}_2 &= (d_S d_V - \Lambda_V \beta_1)\big(\beta_2 \Lambda_A (\gamma + d_I + \alpha) + \beta_2 \kappa \Lambda_A \theta\big) \\
&\quad - \Lambda_V \beta_2 \varepsilon \beta_1 \Lambda_S (\gamma + d_I + \alpha - \kappa\theta) + d_S d_V^2 (\gamma + d_I + \alpha)(d_A + \theta), \\
\mathscr{A}_3 &= -d_S \Lambda_V \beta_2 \Lambda_A (\gamma + d_I + \alpha).
\end{aligned}$$

Since $\mathscr{A}_1 > 0$ and $\mathscr{A}_3 < 0$, the quadratic equation admits exactly one positive root given by the following:

$$I_V^* = \frac{-\mathscr{A}_2 + \sqrt{\mathscr{A}_2^2 - 4\mathscr{A}_1\mathscr{A}_3}}{2\mathscr{A}_1}. \tag{D.11}$$

Therefore, the model admits a unique strictly positive endemic equilibrium.

E. Proof of Theorem 5.1

Proof. Following the methodology outlined in [59], we establish a Lyapunov function for systems (2.1)–(2.6) at the endemic equilibrium E^*. Define the Lyapunov function as follows:

$$L = S^*\phi\left(\frac{S}{S^*}\right) + I^*\phi\left(\frac{I}{I^*}\right) + A^*\phi\left(\frac{A}{A^*}\right) + \left(\frac{(d_A+\theta)A^*}{\varepsilon\beta_2 S_V^* A^*}\right) S_V^*\phi\left(\frac{S_V}{S_V^*}\right) + \left(\frac{(d_A+\theta)A^*}{\varepsilon\beta_2 S_V^* A^*}\right) I_V^*\phi\left(\frac{I_V}{I_V^*}\right). \tag{E.1}$$

We assume that the function ϕ is defined by the following:

$$\phi(y) = y - 1 - \ln(y),$$

which is defined on $\mathbb{R}_+^*$ and admits a strict global minimum equal to zero. These properties of ϕ play a crucial role in the Lyapunov stability analysis. The time derivative of the Lyapunov function L along the trajectories of the system is given by

$$\dot{L} = (1 - \frac{S^*}{S})\dot{S} + (1 - \frac{A^*}{A})\dot{A} + (1 - \frac{I^*}{I})\dot{I} + ((\frac{d_A + \theta}{\varepsilon})A^*)(1 - \frac{S_V^*}{S_V})\dot{S_V} + ((\frac{d_A + \theta}{\varepsilon})A^*)(1 - \frac{I_V^*}{I_V})\dot{I_V}. \quad \text{(E.2)}$$

Each term that appears in $\dot{L}$ can be rewritten as follows:

$$\begin{aligned}
\left(1 - \frac{S^*}{S}\right)\dot{S} &= \left(1 - \frac{S^*}{S}\right)(\Lambda_S - d_S S - \beta_1 S I_V) \\
&= \left(1 - \frac{S^*}{S}\right)(d_S S^* + \beta_1 S^* I_V^* - d_S S - \beta_1 S I_V) \\
&= -d_S \frac{(S - S^*)^2}{S} + \beta_1 S^* I_V^* \left(1 - \frac{S I_V}{S^* I_V^*}\right)\left(1 - \frac{S^*}{S}\right) \\
&= -d_S \frac{(S - S^*)^2}{S} + \beta_1 S^* I_V^* \left(1 - \frac{S I_V}{S^* I_V^*} - \frac{S^*}{S} + \frac{I_V}{I_V^*}\right) \\
&= -d_S \frac{(S - S^*)^2}{S} + \beta_1 S^* I_V^* \left(-\phi\left(\frac{S I_V}{S^* I_V^*}\right) - \phi\left(\frac{S^*}{S}\right) + \phi\left(\frac{I_V}{I_V^*}\right)\right).
\end{aligned} \quad \text{(E.3)}$$

$$\begin{aligned}
\left(1 - \frac{A^*}{A}\right)\dot{A} &= \left(1 - \frac{A^*}{A}\right)(\Lambda_A - (d_A + \theta)A + \varepsilon\beta_1 S I_V) \\
&= \left(1 - \frac{A^*}{A}\right)\left(\Lambda_A + \varepsilon\beta_1 S I_V - \frac{\Lambda_A + \varepsilon\beta_1 S^* I_V^*}{A^*} A\right) \\
&= \left(1 - \frac{A^*}{A}\right)\left(\Lambda_A - \frac{\Lambda_A A}{A^*}\right) + \left(1 - \frac{A^*}{A}\right)\left(\varepsilon\beta_1 S I_V - \frac{\varepsilon\beta_1 S^* I_V^* A}{A^*}\right) \\
&= -\Lambda_A \frac{(A - A^*)^2}{A A^*} + \varepsilon\beta_1 S^* I_V^* \left(\frac{S I_V}{S^* I_V^*} - \frac{A}{A^*} - \frac{A^* S I_V}{A S^* I_V^*} + 1\right) \\
&= -\Lambda_A \frac{(A - A^*)^2}{A A^*} + \varepsilon\beta_1 S^* I_V^* \left(\phi\left(\frac{S I_V}{S^* I_V^*}\right) - \phi\left(\frac{A}{A^*}\right) - \phi\left(\frac{A^* S I_V}{A S^* I_V^*}\right)\right).
\end{aligned} \quad \text{(E.4)}$$

$$
\begin{aligned}
\left(1-\frac{I^*}{I}\right)\dot{I} &= \left(1-\frac{I^*}{I}\right)\Big((1-\varepsilon)\beta_1 SI_V + \theta A - (\gamma+d_I+\alpha)I\Big) \\
&= \left(1-\frac{I^*}{I}\right)\left((1-\varepsilon)\beta_1 SI_V + \theta A - \frac{(1-\varepsilon)\beta_1 S^* I_V^*}{I^*} I - \frac{\theta A^*}{I^*} I\right) \\
&= (1-\varepsilon)\beta_1 S^* I_V^* \left(\frac{SI_V}{S^* I_V^*} - \frac{I}{I^*} - \frac{I^* SI_V}{I S^* I_V^*} + 1\right) \\
&\quad + \theta A^* \left(\frac{A}{A^*} - \frac{I}{I^*} - \frac{AI^*}{IA^*} + 1\right) \\
&= (1-\varepsilon)\beta_1 S^* I_V^* \left(\phi\left(\frac{SI_V}{S^* I_V^*}\right) - \phi\left(\frac{I}{I^*}\right) - \phi\left(\frac{I^* SI_V}{I S^* I_V^*}\right)\right) \\
&\quad + \theta A^* \left(\phi\left(\frac{A}{A^*}\right) - \phi\left(\frac{I}{I^*}\right) - \phi\left(\frac{AI^*}{IA^*}\right)\right).
\end{aligned}
\tag{E.5}
$$

$$
\begin{aligned}
(1-\tfrac{S_V^*}{S_V})\dot{S_V} &= (1-\tfrac{S_V^*}{S_V})(\beta_2 S_V(A^*+\kappa I^*) + d_V S_V^* - \beta_2 S_V(A+\kappa I) - d_V S_V) \\
&= (1-\tfrac{S_V^*}{S_V})(\beta_2 S_V^* A^* - \beta_2 S_V A) + (1-\tfrac{S_V^*}{S_V})(\beta_2 \kappa S_V^* I^* - \beta_2 \kappa S_V I) \\
&\quad + (1-\tfrac{S_V^*}{S_V})(d_V S_V^* - d_V S_V) \\
&= -d_V \tfrac{(S_V^*-S_V)^2}{S_V} + \beta_2 \kappa S_V^* I^* \left(1 - \tfrac{S_V I}{S_V^* I^*} + \tfrac{S_V^*}{S_V} + \tfrac{I}{I^*}\right) \\
&\quad + \beta_2 S_V^* A^* \left(1 - \tfrac{S_V A}{S_V^* A^*} - \tfrac{S_V^*}{S_V} + \tfrac{A}{A^*}\right) \\
&= -d_V \tfrac{(S_V^*-S_V)^2}{S_V} + \beta_2 \kappa S_V^* I^* \left(-\phi\left(\tfrac{S_V I}{S_V^* I^*}\right) + \phi\left(\tfrac{S_V^*}{S_V}\right) + \phi\left(\tfrac{I}{I^*}\right)\right) \\
&\quad + \beta_2 S_V^* A^* \left(-\phi\left(\tfrac{S_V A}{S_V^* A^*}\right) - \phi\left(\tfrac{S_V^*}{S_V}\right) + \phi\left(\tfrac{A}{A^*}\right)\right). \\
(1-\tfrac{I_V^*}{I_V})\dot{I_V} &= (1-\tfrac{I_V^*}{I_V})(\beta_2 S_V A + \beta_2 \kappa S_V I - d_V I_V) \\
&= (1-\tfrac{I_V^*}{I_V})(\beta_2 S_V A + \beta_2 S_V I - \tfrac{\beta_2 S_V^* A^* I_V}{I_V^*} - \tfrac{\beta_2 \kappa S_V^* I_V I^*}{I_V^*}) \\
&= \beta_2 S_V^* A^* (\tfrac{S_V A}{S_V^* A^*} - \tfrac{I_V}{I_V^*} - \tfrac{I_V^* S_V A}{I_V S_V^* A^*} + 1) + \beta_2 \kappa S_V^* I^* (\tfrac{S_V I}{S_V^* I^*} - \tfrac{I_V}{I_v^*} - \tfrac{I_V^* S_V I}{S_V^* I^* I_V} + 1) \\
&= \beta_2 S_V^* A^* \left(\phi\left(\tfrac{S_V A}{S_V^* A^*}\right) - \phi\left(\tfrac{I_V}{I_V^*}\right) - \phi\left(\tfrac{I_V^* S_V A}{I_V S_V^* A^*}\right)\right) \\
&+ \beta_2 \kappa S_V^* I^* \left(\phi\left(\tfrac{S_V I}{S_V^* I^*}\right) - \phi\left(\tfrac{I_V}{I_v^*}\right) - \phi\left(\tfrac{I_V^* S_V I}{S_V^* I^* I_V}\right)\right).
\end{aligned}
$$

Now, the time derivative of the Lyapunov function can be expressed as follows:

$$\begin{aligned}
\dot{L} = &\left(-d_S\frac{(S^*-S)^2}{S}+\beta_1 I_V^* S^*\left[-\phi\left(\frac{SI_V}{S^*I_V^*}\right)-\phi\left(\frac{S^*}{S}\right)+\phi\left(\frac{I_V}{I_V^*}\right)\right]\right)\\
&+\left(-\Lambda_A\frac{(A-A^*)^2}{AA^*}+\varepsilon\beta_1 S^* I_V^*\left[\phi\left(\frac{SI_V}{S^*I_V^*}\right)-\phi\left(\frac{A}{A^*}\right)-\phi\left(\frac{A^*SI_V}{AS^*I_V^*}\right)\right]\right)\\
&+\left((1-\varepsilon)\beta_1 SI_V\left[\phi\left(\frac{SI_V}{S^*I_V^*}\right)-\phi\left(\frac{I}{I^*}\right)-\phi\left(\frac{I^*SI_V}{IS^*I_V^*}\right)\right]\right.\\
&\quad\left.+\theta A^*\left[\phi\left(\frac{A}{A^*}\right)-\phi\left(\frac{I}{I^*}\right)-\phi\left(\frac{AI^*}{IA^*}\right)\right]\right)\\
&+\left(\frac{d_A+\theta}{\varepsilon}A^*\right)\left(-d_V\frac{(S_V^*-S_V)^2}{S_V}\right.\\
&\quad+\beta_2\kappa S_V^* I^*\left[-\phi\left(\frac{S_V I}{S_V^* I^*}\right)+\phi\left(\frac{S_V^*}{S_V}\right)+\phi\left(\frac{I}{I^*}\right)\right]\\
&\quad\left.+\beta_2 S_V^* A^*\left[-\phi\left(\frac{S_V A}{S_V^* A^*}\right)-\phi\left(\frac{S_V^*}{S_V}\right)+\phi\left(\frac{A}{A^*}\right)\right]\right)\\
&+C_5\left(\beta_2 S_V^* A^*\left[\phi\left(\frac{S_V A}{S_V^* A^*}\right)-\phi\left(\frac{I_V}{I_V^*}\right)-\phi\left(\frac{I_V^* S_V A}{I_V S_V^* A^*}\right)\right]\right.\\
&\quad\left.+\beta_2\kappa S_V^* I^*\left[\phi\left(\frac{S_V I}{S_V^* I^*}\right)-\phi\left(\frac{I_V}{I_V^*}\right)-\phi\left(\frac{I_V^* S_V I}{S_V^* I^* I_V}\right)\right]\right).
\end{aligned}$$

We recall that $0<\varepsilon<1$, which implies $0<1-\varepsilon<1$. Consequently,

$$\varepsilon\beta_1 S^* I_V^* < \beta_1 S^* I_V^*, \qquad (1-\varepsilon)\beta_1 S^* I_V^* < \beta_1 S^* I_V^*.$$

Moreover, since

$$A^* = \frac{1}{d_A+\theta}\left(\Lambda_A+\frac{\varepsilon\beta_1\Lambda_S I_V^*}{d_S+\beta_1 I_V^*}\right), \qquad S^* = \frac{\Lambda_S}{d_S+\beta_1 I_V^*},$$

we obtain

$$\theta A^* > \frac{\theta\varepsilon\beta_1 S^* I_V^*}{d_A+\theta}, \quad \text{and hence} \quad \frac{(d_A+\theta)A^*}{\varepsilon} > \beta_1 S^* I_V^*.$$

In addition, we note that

$$(d_A+\theta)A^* > \theta A^*, \qquad (d_A+\theta)A^* < \left(\frac{d_A+\theta}{\varepsilon}\right)A^*,$$

and

$$\beta_2\kappa S_V^* I^* = \frac{\beta_2\kappa S_V^*\theta A^*}{\gamma+d_I+\alpha}.$$

Additionally, it is important to observe that the terms

$$-d_S\frac{(S^*-S)^2}{S},\quad -\Lambda_A\frac{(A-A^*)^2}{AA^*},\quad -d_V\frac{(S_V^*-S_V)^2}{S_V}$$

are all strictly negative.

Having established the above inequalities, we incorporate all terms to finalize the computation of $\dot{L}$. We obtain the following:

$$\begin{aligned}
\dot{L} \leq\ & \left(\left(\tfrac{d_A+\theta}{\varepsilon}\right)A^*\right)\left(-\phi\left(\tfrac{SI_V}{S^*I_V^*}\right)-\phi\left(\tfrac{S^*}{S}\right)+\phi\left(\tfrac{I_V}{I_V^*}\right)\right)\\
+\ & \left(\left(\tfrac{d_A+\theta}{\varepsilon}\right)A^*\right)\left(\phi\left(\tfrac{SI_V}{S^*I_V^*}\right)-\phi\left(\tfrac{A}{A^*}\right)-\phi\left(\tfrac{A^*SI_V}{AS^*I_V^*}\right)\right)\\
+\ & \left(\left(\tfrac{d_A+\theta}{\varepsilon}\right)A^*\right)\left(\phi\left(\tfrac{SI_V}{S^*I_V^*}\right)-\phi\left(\tfrac{I}{I^*}\right)-\phi\left(\tfrac{I^*SI_V}{IS^*I_V^*}\right)+\phi\left(\tfrac{A}{A^*}\right)-\phi\left(\tfrac{I}{I^*}\right)-\phi\left(\tfrac{AI^*}{IA^*}\right)\right)\\
+\ & \left(\left(\tfrac{d_A+\theta}{\varepsilon}\right)A^*\right)\left(\tfrac{\beta_2\kappa S_V^*\theta A^*}{\gamma+d_I+\alpha}\right)\left(-\phi\left(\tfrac{S_VI}{S_V^*I^*}\right)+\phi\left(\tfrac{S_V^*}{S_V}\right)+\phi\left(\tfrac{I}{I^*}\right)\right)\\
+\ & C_4\beta_2S_V^*A^*\left(-\phi\left(\tfrac{S_VA}{S_V^*A^*}\right)-\phi\left(\tfrac{S_V^*}{S_V}\right)+\phi\left(\tfrac{A}{A^*}\right)\right)\\
+\ & C_5\beta_2S_V^*A^*\left(\phi\left(\tfrac{S_VA}{S_V^*A^*}\right)-\phi\left(\tfrac{I_V}{I_V^*}\right)-\phi\left(\tfrac{I_V^*S_VA}{I_VS_V^*A^*}\right)\right)\\
+\ & \left(\left(\tfrac{d_A+\theta}{\varepsilon}\right)A^*\right)\tfrac{\beta_2\kappa S_V^*\theta A^*}{\gamma+d_I+\alpha}\left(\phi\left(\tfrac{S_VI}{S_V^*I^*}\right)-\phi\left(\tfrac{I_V}{I_v^*}\right)-\phi\left(\tfrac{I_V^*S_VI}{S_V^*I^*I_V}\right)\right).
\end{aligned}$$

Therefore, the derivative of the Lyapunov function satisfies the following:

$$\begin{aligned}
\dot{L} \leq\ & \left(\left(\tfrac{d_A+\theta}{\varepsilon}\right)A^*\right)\left(\phi\left(\tfrac{SI_V}{S^*I_V^*}\right)-\phi\left(\tfrac{I_V}{I_V^*}\right)-\phi\left(\tfrac{S^*}{S}\right)-\phi\left(\tfrac{A^*SI_V}{AS^*I_V^*}\right)-\phi\left(\tfrac{I}{I^*}\right)-\phi\left(\tfrac{I_VSI^*}{I_V^*S^*I}\right)\right.\\
-\ & \left.\phi\left(\tfrac{AI^*}{A^*I}\right)+\phi\left(\tfrac{A}{A^*}\right)-\phi\left(\tfrac{I_V^*S_VA}{I_VS_V^*A^*}\right)\right).
\end{aligned}$$

We have that

$$\begin{aligned}
&\left(\phi\left(\tfrac{SI_V}{S^*I_V^*}\right)-\phi\left(\tfrac{I_V}{I_V^*}\right)-\phi\left(\tfrac{S^*}{S}\right)-\phi\left(\tfrac{A^*SI_V}{AS^*I_V^*}\right)-\phi\left(\tfrac{I}{I^*}\right)-\phi\left(\tfrac{I_V^*S_VA}{I_VS_V^*A^*}\right)-\phi\left(\tfrac{AI^*}{A^*I}\right)\right.\\
&\left.-\phi\left(\tfrac{I_V^*S_VI}{I_VS_V^*I^*}\right)-\phi\left(\tfrac{I^*SI_V}{IS^*I_V^*}\right)+\phi\left(\tfrac{A}{A^*}\right)\right)\leq 0.
\end{aligned}$$

Indeed,

$$\phi\left(\tfrac{A}{A^*}\right)-\phi\left(\tfrac{AI^*}{IA^*}\right) = \tfrac{A}{A^*}-\tfrac{AI^*}{A^*I}+\ln\left(\tfrac{I^*}{I}\right).$$

Since $\phi\left(\frac{I^*}{I}\right) \geq 0$, it follows that

$$\ln\left(\frac{I^*}{I}\right) \leq \frac{I^*}{I} - 1.$$

Hence,

$$\begin{aligned}
\phi\left(\tfrac{A}{A^*}\right) - \phi\left(\tfrac{AI^*}{IA^*}\right) &\leq \tfrac{A}{A^*}\left(1 - \tfrac{I^*}{I}\right) - 1 + \tfrac{I^*}{I}, \\
\phi\left(\tfrac{A}{A^*}\right) - \phi\left(\tfrac{AI^*}{IA^*}\right) &\leq -\left(\tfrac{I^*}{I} - 1\right)\left(\tfrac{A}{A^*} - 1\right).
\end{aligned}$$

Using the same technique for $\phi\left(\frac{SI_V}{S^*I_V^*}\right) - \phi\left(\frac{I^*SI_V}{IS^*I_v^*}\right)$, we obtain the following:

$$\phi\left(\tfrac{SI_V}{S^*I_V^*}\right) - \phi\left(\tfrac{I^*SI_V}{IS^*I_v^*}\right) \leq -\left(\tfrac{I^*}{I} - 1\right)\left(\tfrac{SI_V}{S^*I_V^*} - 1\right).$$

By using $(\mathbf{H}_2)$, we conclude that

$$\begin{aligned}
\phi\left(\tfrac{A}{A^*}\right) - \phi\left(\tfrac{AI^*}{IA^*}\right) &\leq 0, \\
\phi\left(\tfrac{SI_V}{S^*I_V^*}\right) - \phi\left(\tfrac{I^*SI_V}{IS^*I_v^*}\right) &\leq 0.
\end{aligned}$$

Finally, we conclude that $\dot{L} \leq 0$. According to LaSalle's invariance principle [60], the endemic equilibrium E^* is globally asymptotically stable.

F. Proof of Theorem 7.2

Proof. By applying Pontryagin's Maximum Principle in conjunction with the Hamiltonian defined in (7.11), and introducing the following variable substitutions, we obtain the following:

$$\begin{aligned}
\dot{\lambda}_1(t) &= -\frac{\partial H(t)}{\partial S(t)} = \lambda_1 d_S + (1-u_2)\beta_1 I_V(\lambda_1 - \lambda_3) + (1-u_2)\varepsilon\beta_1 I_V(\lambda_3 - \lambda_2), \\
\dot{\lambda}_2(t) &= -\frac{\partial H(t)}{\partial A(t)} = d_A\lambda_2 + \theta(\lambda_2 - \lambda_3) + \beta_2 S_V(1-u_2)(\lambda_5 - \lambda_6), \\
\dot{\lambda}_3(t) &= -\frac{\partial H(t)}{\partial I(t)} = -D_1 + \lambda_3(d_I + \alpha) + (\gamma + u_3)(\lambda_3 - \lambda_4) + \beta_2 S_V(1-u_2)\kappa(\lambda_5 - \lambda_6), \\
\dot{\lambda}_4(t) &= -\frac{\partial H(t)}{\partial R(t)} = d_R\lambda_4, \\
\dot{\lambda}_5(t) &= -\frac{\partial H(t)}{\partial S_V(t)} = \beta_2(1-u_2)(A + \kappa I)(\lambda_5 - \lambda_6) + (d_V + u_4)\lambda_5, \\
\dot{\lambda}_6(t) &= -\frac{\partial H(t)}{\partial I_V(t)} = -D_2 + (1-u_2)\beta_1 S I_V(\lambda_1 - \varepsilon\lambda_2 - (1-\varepsilon)\lambda_3) + (d_V + u_4)\lambda_6.
\end{aligned} \tag{F.1}$$

Applying the optimality conditions, we obtain the following:

$$\begin{aligned}
\frac{\partial H(t)}{\partial u_1(t)} &= B_1 u_1 - \lambda_1 \Lambda_S - \lambda_2 \Lambda_A - \lambda_4 \Lambda_R, \\
\frac{\partial H(t)}{\partial u_2(t)} &= B_2 u_2 + \beta_1 S I_V \left[\lambda_1 - \varepsilon\lambda_2 - (1-\varepsilon)\lambda_3\right] + \beta_2 S_V (A + \kappa I)\left[\lambda_5 - \lambda_6\right], \\
\frac{\partial H(t)}{\partial u_3(t)} &= B_3 u_3 + I\left(\lambda_4 - \lambda_3\right), \\
\frac{\partial H(t)}{\partial u_4(t)} &= B_4 u_4 - \lambda_5 S_V - \lambda_6 I_V.
\end{aligned} \tag{F.2}$$

Thus, setting $\frac{\partial H(t)}{\partial u_i(t)} = 0$ for $i = 1, \ldots, 4$ yields the following:

$$\frac{\partial H(t)}{\partial u_1(t)} = 0 \quad \text{Implies} \quad u_1^* = \frac{\lambda_1 \Lambda_S + \lambda_2 \Lambda_A + \lambda_4 \Lambda_R}{B_1}, \tag{F.3}$$

$$\frac{\partial H(t)}{\partial u_2(t)} = 0 \quad \text{Implies} \quad u_2^* = \frac{\beta_1 S I_V \left(\varepsilon\lambda_2 + (1-\varepsilon)\lambda_3 - \lambda_1\right) + \beta_2 S_V (A + \kappa I)\left(\lambda_5 - \lambda_6\right)}{B_2}, \tag{F.4}$$

$$\frac{\partial H(t)}{\partial u_3(t)} = 0 \quad \text{Implies} \quad u_3^*(t) = \frac{I(\lambda_3 - \lambda_4)}{B_3}. \tag{F.5}$$

$$\frac{\partial H(t)}{\partial u_4(t)} = 0 \quad \text{Implies} \quad u_4^*(t) = \frac{\lambda_5 S_V + \lambda_6 I_V}{B_4}. \tag{F.6}$$

Hence, applying the control bounds yields the following:

$$u_1^* = \begin{cases} 0 & \text{if } \dfrac{\lambda_1 \Lambda_S + \lambda_2 \Lambda_A + \lambda_4 \Lambda_R}{B_1} \leq 0, \\ \dfrac{\lambda_1 \Lambda_S + \lambda_2 \Lambda_A + \lambda_4 \Lambda_R}{B_1} & \text{if } 0 < \dfrac{\lambda_1 \Lambda_S + \lambda_2 \Lambda_A + \lambda_4 \Lambda_R}{B_1} < 1, \\ 1 & \text{if } \dfrac{\lambda_1 \Lambda_S + \lambda_2 \Lambda_A + \lambda_4 \Lambda_R}{B_1} \geq 1. \end{cases} \tag{F.7}$$

$$u_2^* = \begin{cases} 0 & \text{if } \dfrac{\beta_1 S I_V \left(\varepsilon\lambda_2 + (1-\varepsilon)\lambda_3 - \lambda_1\right) + \beta_2 S_V (A + \kappa I)(\lambda_6 - \lambda_5)}{B_2} \leq 0, \\ \dfrac{\beta_1 S I_V \left(\varepsilon\lambda_2 + (1-\varepsilon)\lambda_3 - \lambda_1\right) + \beta_2 S_V (A + \kappa I)(\lambda_6 - \lambda_5)}{B_2} & \text{if } 0 < \dfrac{\beta_1 S I_V \left(\varepsilon\lambda_2 + (1-\varepsilon)\lambda_3 - \lambda_1\right) + \beta_2 S_V (A + \kappa I)(\lambda_6 - \lambda_5)}{B_2} < 1, \\ 1 & \text{if } \dfrac{\beta_1 S I_V \left(\varepsilon\lambda_2 + (1-\varepsilon)\lambda_3 - \lambda_1\right) + \beta_2 S_V (A + \kappa I)(\lambda_6 - \lambda_5)}{B_2} \geq 1. \end{cases} \tag{F.8}$$

$$u_3^* = \begin{cases} 0 & \text{if } \dfrac{I(\lambda_3-\lambda_4)}{B_3} \le 0, \\ \dfrac{I(\lambda_3-\lambda_4)}{B_3} & \text{if } 0 < \dfrac{I(\lambda_3-\lambda_4)}{B_3} < 1, \\ 1 & \text{if } \dfrac{I(\lambda_3-\lambda_4)}{B_3} \ge 1. \end{cases} \tag{F.9}$$

$$u_4^* = \begin{cases} 0 & \text{if } \dfrac{\lambda_5 S_V + \lambda_6 I_V}{B_4} \le 0, \\ \dfrac{\lambda_5 S_V + \lambda_6 I_V}{B_4} & \text{if } 0 < \dfrac{\lambda_5 S_V + \lambda_6 I_V}{B_4} < 1, \\ 1 & \text{if } \dfrac{\lambda_5 S_V + \lambda_6 I_V}{B_4} \ge 1. \end{cases} \tag{F.10}$$

Therefore, we obtain the following characterization of the optimal controls, based on the admissible control set:

$$\begin{aligned} u_1^* &= \max\left\{\min\left(\tfrac{\lambda_1\Lambda_S+\lambda_2\Lambda_A+\lambda_4\Lambda_R}{B_1}, 1\right), 0\right\}, \\ u_2^* &= \max\left\{\min\left(\tfrac{\beta_1 S I_V(\varepsilon\lambda_2+(1-\varepsilon)\lambda_3-\lambda_1)+\beta_2 S_V(A+\kappa I)(\lambda_5-\lambda_6)}{B_2}, 1\right), 0\right\}, \\ u_3^* &= \max\left\{\min\left(\tfrac{I(\lambda_3-\lambda_4)}{B_3}, 1\right), 0\right\}, \\ u_4^* &= \max\left\{\min\left(\tfrac{\lambda_5 S_V+\lambda_6 I_V}{B_4}, 1\right), 0\right\}. \end{aligned} \tag{F.11}$$

AIMS Press

© 2026 the Author(s), licensee AIMS Press. This is an open access article distributed under the terms of the Creative Commons Attribution License (https://creativecommons.org/licenses/by/4.0)